An Actin-Binding Protein, LlLIM1, Mediates Calcium and Hydrogen Regulation of Actin Dynamics in Pollen Tubes[1][C][W][OA]

Huei-Jing Wang, Ai-Ru Wan, and Guang-Yuh Jauh*

Institute of Plant and Microbial Biology, Academia Sinica, Nankang, Taipei 115, Taiwan, Republic of China (H.-J.W., A.-R.W., G.-Y.J); and Institute of Life Science, National Defense Medical Center, Taipei 114, Taiwan, Republic of China (H.-J.W.)

Actin microfilaments are crucial for polar cell tip growth, and their configurations and dynamics are regulated by the actions of various actin-binding proteins (ABPs). We explored the function of a lily (*Lilium longiflorum*) pollen-enriched LIM domain-containing protein, LlLIM1, in regulating the actin dynamics in elongating pollen tube. Cytological and biochemical assays verified LlLIM1 functioning as an ABP, promoting filamentous actin (F-actin) bundle assembly and protecting F-actin against latrunculin B-mediated depolymerization. Overexpressed LlLIM1 significantly disturbed pollen tube growth and morphology, with multiple tubes protruding from one pollen grain and coaggregation of FM4-64-labeled vesicles and Golgi apparatuses at the subapex of the tube tip. Moderate expression of LlLIM1 induced an oscillatory formation of asterisk-shaped F-actin aggregates that oscillated with growth period but in different phases at the subapical region. These results suggest that the formation of LlLIM1-mediated overstabilized F-actin bundles interfered with endomembrane trafficking to result in growth retardation. Cosedimentation assays revealed that the binding affinity of LlLIM1 to F-actin was simultaneously regulated by both pH and Ca^{2+}: LlLIM1 showed a preference for F-actin binding under low pH and low Ca^{2+} concentration. The potential functions of LlLIM1 as an ABP sensitive to pH and calcium in integrating endomembrane trafficking, oscillatory pH, and calcium circumstances to regulate tip-focused pollen tube growth are discussed.

Pollen is the male gametophyte of seed plants, and well-programmed pollen development, germination, and tube growth are essential for successful fertilization. Pollen tube growth is a typical tip-extending process that exhibits highly polarized vesicle secretion and reverse-fountain cytoplasmic streaming, with rapidly moving granular elements seen behind a clear zone at the apical dome of the tube (Hepler et al., 2001; Cheung and Wu, 2008). Many signaling factors have been identified to play essential roles in pollen germination and tube growth, including Rop-GTPases, phospholipase C (PLC), and ions. Their individual functions or cross talk with different pathways coordinate a large, complex signaling network to regulate normal pollen tube growth via vesicle targeting/fusion, cytoskeletal organization, cell wall assembly, and extracellular communication (Malhó, 2006; Cheung and Wu, 2008).

Cytoskeletal actin microfilament (F-actin) is the fundamental element essential for tip extension of polar cells, and precise regulation of its dynamics is critical to conduct its biological functions (Hussey et al., 2006; Staiger and Blanchoin, 2006). For example, disruption of F-actin with the actin polymerization inhibitor latrunculin B (LatB) prohibited pollen tube growth by disturbing organelle movement and continuous transport of cell wall precursors to the tube tip (Chen et al., 2007; Lovy-Wheeler et al., 2007). Promoting and stabilizing F-actin polymerization by jasplakinolide, a sponge cyclodepsipeptide, also blocked cytoplasmic streaming in the shank of the tube and impaired pollen tube growth (Cardenas et al., 2005). Vesicle trafficking driven by F-actin in the clear zone is important for pollen tube elongation. Secretory vesicles carrying membrane and cell wall materials are derived from trans-Golgi networks (TGNs) and transported to apical plasma membranes to deliver their cargo during pollen tube elongation (Šamaj et al., 2006). Pollen tubes stained with FM4-64, a vital styryl dye for the endocytic membrane, revealed inverted cone-shaped staining in the apical clear zone enriched with endocytic and exocytic vesicles (Parton et al., 2001). Brefeldin A (BFA), an inhibitor of the secretory pathway through endosome and TGNs, effectively impaired pollen tube elongation by aggregating secretory vesicles to form

[1] This work was supported by research grants from Academia Sinica (Taiwan), the Taiwan National Science Council (grant nos. 94–2311–B–001–054 and 96–2311–B–001–023–MY3), and the Li Foundation to G.-Y.J.

* Corresponding author; e-mail jauh@gate.sinica.edu.tw.

The author responsible for distribution of materials integral to the findings presented in this article in accordance with the policy described in the Instructions for Authors (www.plantphysiol.org) is: Guang-Yuh Jauh (jauh@gate.sinica.edu.tw).

[C] Some figures in this article are displayed in color online but in black and white in the print edition.

[W] The online version of this article contains Web-only data.

[OA] Open Access articles can be viewed online without a subscription.

www.plantphysiol.org/cgi/doi/10.1104/pp.108.118604

large clusters in an actin-dependent process (Parton et al., 2001; Hörmanseder et al., 2005). Recently, diacyl glycerol (DAG) was found to be internalized from the lateral membrane of the tube tip and retargeted to the apical membrane, a process significantly blocked by BFA (Helling et al., 2006). These studies suggest that complex membrane-trafficking processes controlled by F-actin in the clear zone are critical for normal pollen tube extension.

Pollen tube elongation also exhibits a unique nonlinear pulse and sustained oscillation, which is simultaneously correlated with oscillatory changes of pH and cytosolic Ca^{2+} concentration ($[Ca^{2+}]_c$), in the apical region of pollen tubes. Growing lily (*Lilium longiflorum*) pollen tubes showed tip-focused $[Ca^{2+}]_c$ gradient oscillation during tube growth: in the extreme apical region, the changes in $[Ca^{2+}]_c$ level can be as much as 4-fold (700 to >3,000 nM) during oscillatory growth; at the subapical region, 20 μm away from the extreme apex, $[Ca^{2+}]_c$ gradually decreases to the basal level (150–300 nM; Pierson et al., 1996; Holdaway-Clarke et al., 1997). Microinjected pH-sensitive dye revealed that lily pollen tubes possess an intracellular pH gradient with slightly acidic (pH 6.8) and alkaline (pH 7.5) bands in the apex and subapex regions, respectively, and an oscillating pH change in the apical domain relative to growth (Feijó et al., 1999). However, the pH gradient oscillates during growth but in different phases: increased apical pH precedes the fastest growth velocity, whereas decreased pH follows oscillatory growth (Lovy-Wheeler et al., 2006).

In eukaryotic cells, F-actin configuration and dynamics are accurately regulated via the actions of numerous actin-binding proteins (ABPs) in several aspects, including nucleation, polymerization/depolymerization, stabilization, filament capping, fragmentation, and monomer availability, as well as the establishment of the actin network and bundles (Hussey et al., 2006; Staiger and Blanchoin, 2006). Some ABPs have been identified and characterized in plant cells, especially in pollen tubes. For example, two lily pollen villins, P-115-ABP (Nakayasu et al., 1998) and P-135-ABP (Yokota et al., 1998), assemble F-actin into bundles with uniform polarity, which was suppressed by calcium and calmodulin (Yokota et al., 2000). A *Papaver rhoeas* pollen gelsolin-like protein, PrABP80, functioned as an effective actin nucleator in basal calcium conditions, but it severed and depolymerized actin filaments under high calcium conditions (Huang et al., 2004). A maize (*Zea mays*) profilin, ZmPRO1, a G-actin-binding protein abundant in pollen, sequestered G-actin under high calcium conditions (Kovar et al., 2000). The actin depolymerization factors (ADFs) identified from lily and tobacco (*Nicotiana tabacum*) pollen showed a pH-sensitive F-actin-severing ability. Lily ADF, but not tobacco ADF, together with actin-interacting protein (AIP), stimulated F-actin turnover in a pH-dependent manner (Allwood et al., 2002; Chen et al., 2002). Since the activity of ADF is enhanced under alkaline pH, ADF may be more active around the alkaline band near the tube subapical region, which has a fringe and short actin filaments decorated by ADF, and pH oscillation may regulate pollen tube elongation through controlling actin dynamics (Lovy-Wheeler et al., 2006). All of these results suggest that Ca^{2+} and pH oscillation may regulate actin dynamics to modulate pollen tube growth through the action of these ABPs (Feijó et al., 1999; Staiger and Blanchoin, 2006), but the underlying molecular mechanisms are still unclear.

The LIM domain, consisting of tandem zinc finger motifs, is widely found in various eukaryotic proteins to function as a module for protein-protein interaction (Schmeichel and Beckerle, 1997). Cys-rich proteins (CRPs) are a family of small LIMs of approximately 200 amino acids with two very similar LIM domains separated by a 40- to 50-residue spacer. CRPs are required for terminal differentiation in vertebrate muscle development via their effects on cytoarchitecture and function in both the nucleus and cytoplasm as a transcriptional factor and ABP, respectively (Arber and Caroni, 1996; Khurana et al., 2002). Protein sequence analysis suggests that plant LIMs from Arabidopsis (*Arabidopsis thaliana*), sunflower (*Helianthus annuus*), tobacco, and rice (*Oryza sativa*; Arnaud et al., 2007) belong to the CRP family of animal LIMs (Weiskirchen and Gunther, 2003) also found in the nucleus and cytoplasm (Baltz et al., 1999; Mundel et al., 2000). Recently, Thomas et al. (2006, 2007) showed that tobacco NtWLIM1 functioned as a novel ABP to promote the assembly of rigid F-actin bundles, control actin dynamics, and protect F-actin depolymerization. In this study, we cloned a cDNA encoding a LIM domain-containing protein, *LlLIM1*, from lily pollen tubes. Since actin dynamics is essential for pollen tube growth and NtWLIM1 is critical for the actin cytoskeleton architecture, we speculate that LlLIM1 participates in pollen tube growth through mediating actin dynamics and remodeling. Cellular and biochemical analyses of LlLIM1 protein and its serially deleted variants showed LlLIM1 functioning as a pollen-enriched autonomous ABP to promote F-actin bundling and that both LIM domains were required for its function. Pollen tubes overexpressing LlLIM1 showed retarded pollen germination and tube growth and abnormal morphology, including swollen tubes and multiple tubes protruding from one pollen grain. These phenomena were concurrent with the formation of an abnormal aggregation of asterisk-shaped F-actin and endomembrane structures in the clear zone of slow-growing or nongrowing pollen tubes. Overexpression of LlLIM1 also caused the mislocalization of several signaling molecules, such as phosphatidylinositol-4,5-bisphosphate (PIP2) and DAG, at the apical membrane of elongating pollen tubes. Interestingly, F-actin cosedimentation assay revealed that the actin-binding affinity of LlLIM1 was simultaneously regulated by both pH and Ca^{2+}: LlLIM1 prefers to bind to actin filaments under low pH and low $[Ca^{2+}]$ conditions. We discuss the rational roles of LlLIM1 functioning as an ABP in a

pH- and calcium-sensitive manner in integrating endomembrane trafficking under oscillatory pH and calcium circumstances and growth in the apical region of the pollen tubes.

RESULTS

Cloning and Characterization of LlLIM1, a Lily LIM Isoform Preferentially Expressed in Pollen and Pollen Tubes

We used a homemade lily pollen tube cDNA microarray to screen pollen tube transcripts whose expression levels were upregulated after pollen germination and/or style-secreted exudate treatment (H.-J. Wang, A.-R. Wan, and G.-Y. Jauh, unpublished data). Two cDNAs encoding partial fragments of the LIM domain-containing protein shared high similarity to Arabidopsis AtWLIM1 (Eliasson et al., 2000). A 1,020-bp full-length cDNA (Supplemental Fig. S1A) encoding a 181-amino acid protein, *LlLIM1*, was obtained by 5′ and 3′ RACE, and the expected length was also revealed by northern blotting (Supplemental Fig. S1B). Reverse transcription (RT)-PCR results indicated that *LlLIM1* transcript was widely present in most organs examined, including root, stem, and pistil, but enriched in pollen/pollen tubes (Fig. 1A, top panel). During microspore development, LlLIM1 was present only in mature and desiccated pollen (Fig. 1A, bottom panel). Amino acid sequence alignment analysis (Fig. 1B) showed that LlLIM1 shared high homology with other plant LIMs having two LIM domains, such as AtWLIM1, OsWLIM1 (Arnaud et al., 2007), HaWLIM1 (Baltz et al., 1992), and NtWLIM1 (Eliasson et al., 2000). In addition, for all plant LIMs examined, the tandem zinc finger motifs present in both LIM domains contained eight conserved Cys/His residues (Fig. 1B, asterisks) for zinc binding found in animal LIMs. However, in each zinc finger motif, the pairs of Cys/His residues were separated by 17 amino acid residues, except for the last one in the second LIM domain, which was separated by 15 amino acid residues (Fig. 1B). These results imply that the second LIM domain containing an unusual zinc finger motif may encompass a function different from that of the first LIM domain (see below).

LlLIM1 Functions as an F-Actin-Binding Protein and Promotes F-Actin Bundle Assembly

In tobacco suspension cells, Thomas et al. (2006) suggested that WLIM1 is a novel class of F-actin-binding protein in planta. To examine whether the lily counterpart, LlLIM1, also functions as an ABP in pollen tubes, we transiently expressed *LlLIM1*:*GFP* driven by a maize pollen-specific *ZM13* promoter in lily pollen/pollen tubes. GFP and the mouse mTalin N terminus (Kost et al., 1998) were used as a negative control and an F-actin indicator, respectively. After bombardment, lily pollen was cultured in germination medium for 6 h, and then the localization of these proteins in the elongating

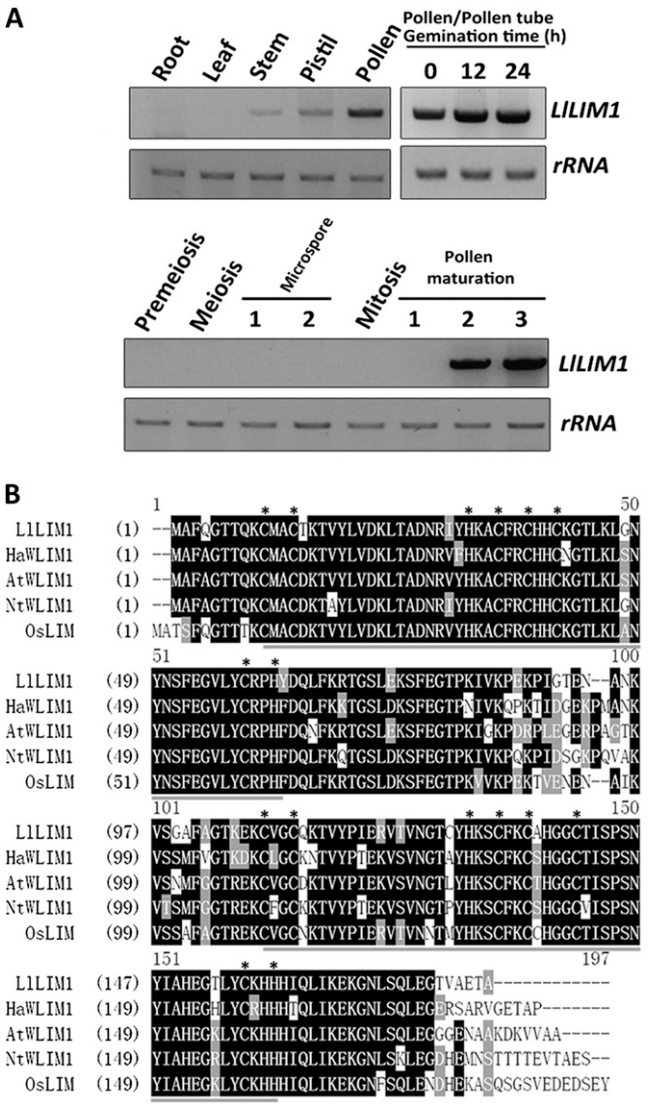

Figure 1. Spatial and temporal expression and protein structure of *LlLIM1*. A, *LlLIM1* expression in different organs and different developmental stages of pollen were determined by semiquantitative RT-PCR. Three micrograms of lily total RNA extracted from root, leaves, stem, pistil, pollen grains, pollen tubes cultured in medium for 12 and 24 h, and anthers collected from flower buds of different lengths (10–20 mm, premeiosis; 20–30 mm, meiosis; 30–45 mm, microspore stage 1; 45–60 mm, microspore stage 2; 60–70 mm, mitosis; 70–90 mm, pollen maturation stage 1; 90–130 mm, pollen maturation stage 2; 130–150 mm, pollen maturation stage 3) were used for reverse transcription to obtain corresponding cDNAs for PCR, with the use of a LlLIM1 coding-region-specific primer set. rRNA amplified by the specific primer set was used as a loading control. B, Alignment analysis of the deduced amino acid sequences of *LlLIM1*, *HaWLIM1* (sunflower; 85.1% similarity and 78.7% identity), *AtWLIM1* (Arabidopsis; 84.7% similarity and 79.5% identity), *NtWLIM1* (tobacco; 81.3% similarity and 76.2% identity), and *OsWLIM1* (rice; 83.1% similarity and 77.9% identity). Black shading, identical and conserved amino acids; gray shading, similar amino acids; dark gray underline, LIM domain; asterisks, identical Cys or His residues for zinc finger motifs.

pollen tube was examined by confocal laser scanning fluorescence microscopy. For pollen tubes cobombarded with *pZM13*::*RFP*:*mTalin* (2.5 μg) and *pZM13*::*GFP* (2.5 μg), GFP was evenly distributed in the cytoplasm and red fluorescent protein (RFP):mTalin decorated the F-actin (Fig. 2A). Pollen tubes cotransformed with 2.5 μg of *pZM13*::*GFP*:*LlLIM1* or *pZM13*::*LlLIM1*:*GFP* plasmid and 2.5 μg of *pZM13*::*RFP*:*mTalin* plasmid showed LlLIM1 colocalizing with mTalin on the F-actin but better decoration of fine and short filaments in apical or subapical regions and longer filaments in the shank region of pollen tubes than with mTalin (Fig. 2, B and C). Recently, several studies suggested that ectopically expressed GFP-mTalin is not a faithful marker and fails to label highly dynamic and dense actin networks in planta (Sheahan et al., 2004; Wang et al., 2004; Voigt et al., 2005), affects the interaction of ADF with F-actin, and results in adverse effects on plant morphology or development (Ketelaar et al., 2004; Voigt et al., 2005). To reveal the reality of LlLIM1 functioning as an ABP, another control, lily pollen-specific LlADF1 (Allwood et al., 2002), was used. Pollen tubes cotransformed with 2.5 μg of *pZM13*::*LlLIM1*:*GFP* and *pZM13*::*LlADF1*:*RFP* plasmids also showed colocalization of LlLIM1 and mTalin on the F-actin (Fig. 2D). In addition, 200 nM LatB treatment completely dispersed the F-actin labeled by LlLIM:GFP and RFP:mTalin (Fig. 2E).

Next, we used purified 6×His-tagged LlLIM1 recombinant protein to examine F-actin-binding activity by cosedimentation assay. After 100,000*g* centrifugation, the recombinant LlLIM1s were present only in the supernatant fraction as soluble proteins, but the commercial rabbit muscle actin filaments were well precipitated (Fig. 2F). Various amounts of LlLIM1 were incubated with 4 μM F-actin and then underwent 100,000*g* centrifugation. As shown in Figure 2G, cosedimentation of recombinant LlLIM1 proteins with F-actin started from 2 μM LlLIM1 and gradually increased up to saturation at approximately 24 μM LlLIM1. To verify the specificity of F-actin affinity, 48 μM bovine serum albumin used as a control revealed no binding activity to F-actin as with LlLIM1 (Fig. 2F). In addition, with low-speed (12,500*g*) sedimentation assay to examine the F-actin-bundling activity of LlLIM1, as reported by Thomas et al. (2006), LlLIM1 was able to bundle F-actin into a high-order cable structure, as evidenced by cosedimentation with F-actin (Fig. 2H). The colocalization of LlLIM1 with mTalin and LlADF1, disruption of their association with F-actin by LatB treatment, and cosedimentation of LlLIM1 with F-actin not only substantiate LlLIM1 functioning as an ABP in elongating pollen tubes but also reveal that LlLIM:GFP will be an exploitable actin marker in living plant cells.

Ectopically Expressed LlLIM1 Showed Adverse Effects on Pollen Tube Elongation and Morphology

To explore the biological function of LlLIM1 in elongating the pollen tube, we performed transiently ectopic overexpression of LlLIM1. After bombardment, lily pollen grains were cultured in germination medium for 12 h, then morphology and F-actin distribution were examined in elongating pollen tubes. As shown in Figure 3, control pollen tubes transformed with GFP showed normal morphology (GFP); however, overexpression of 7.5 μg of LlLIM1:GFP (GFP:LlLIM1) and/or 5 μg of LlLIM1 with 2.5 μg of GFP (LlLIM1+GFP) significantly retarded pollen germination and tube growth. In addition, pollen tubes overexpressing GFP:LlLIM1 (data not shown) and LlLIM1:GFP showed pleiotropic phenotypes: approximately 80% of the transformed pollen tubes were normal with short tube length, but approximately 15% showed a slightly swelled tube tip, and some (approximately 5%) showed a seriously abnormal phenotype with multiple tubes deriving from a single pollen grain (Fig. 3B). Such unique pleiotropic tip phenotypes were not observed with lower dosage treatments. The confocal projection of serial Z-sectioned images showed tubes containing densely labeled filaments and speckles of F-actin in the tip region (Fig. 3C). These dosage-dependent effects strongly suggest that overexpression of LlLIM1 impairs normal pollen tube growth; however, pollen tubes were still capable of resuming normal growth and continuously organizing new growth fronts that eventually turned into a unique phenotype with multiple tubes protruding from single pollen. Analysis of pollen tube length of the transformed pollen tubes confirmed the close correlation of the pollen tube length and dosage of LlLIM1 with short tube length on increased expression of LlLIM1 (Fig. 3D). We noted that the average growth rate of pollen tubes transformed with GFP (approximately 50–150 nm s^{-1}; estimated from Fig. 3D) was shorter than that for untransformed tubes (approximately 200–300 nm s^{-1}; Hepler et al., 2001). To verify whether this variation in growth rates was caused by the different culture conditions or simply the overexpressed chimera proteins, we germinated both GFP- and LlLIM1-transformed pollen tubes in the culture medium used by Holdaway-Clarke et al. (2003) and obtained morphologic features and growth rates comparable to those shown in Figure 3 (data not shown). The above results suggest that overexpressed LlLIM1 interferes with actin dynamics and causes adverse effects on the growth and morphology of pollen tubes.

The First and Second LIM Domains within LlLIM1 Show Different Actin-Binding Efficiency

LlLIM1 contains tandem LIM domains, and primary sequence analysis showed the second zinc finger motif in the second LIM domain containing an unusual zinc finger structure (Fig. 1), which led us to speculate that two LIM domains may have different affinity to F-actin. Individual LIM domains, separated between Asn-93 and Ala-94, and serial deletions of individual LIM domains tagged with GFP in their C termini (Supplemental Fig. S2A) were used to examine their in vivo actin-binding capacities. Among the constructs

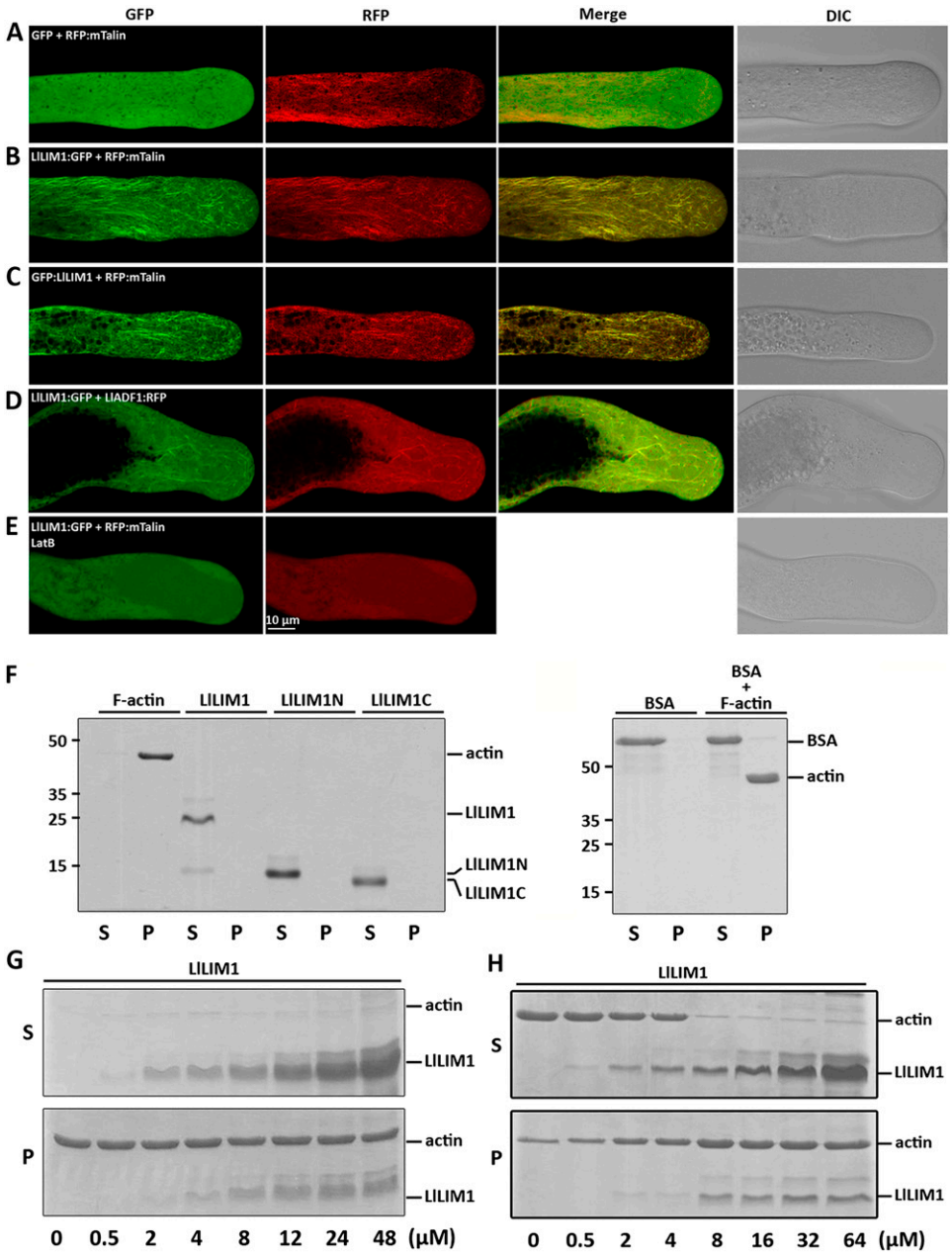

Figure 2. LlLIM1 functions as an ABP in elongating lily pollen tubes and promote F-actin bundling, as revealed by cosedimentation assays. Confocal images show lily pollen tubes coexpressed with *GFP* and *RFP:mTalin* fusion genes (A), *LlLIM1:GFP* and *RFP:mTalin* fusion genes (B), and *GFP:LlLIM1* and *RFP:mTalin* fusion genes (C). The images in D were from the lily pollen tube shown in C, except that the transformed pollen tubes were treated with 200 nM LatB for 1 h before recording the images. In all cases, hydrated pollen grains were cobombarded with 2.5 μg of each indicated plasmid, followed by germination in culture medium for 6 h before images were taken by fluorescent laser scanning confocal microscopy. Different fluorescent channels of images are indicated at the top of the panels. Medial sections through pollen tubes lying flat on the cover-slide surface are shown and represent at least 15 similar images collected from at least three independent experiments. DIC, Differential interference contrast. High- and low-speed cosedimentation assays were used to examine the capability for binding (G) and bundle assembly (H), respectively, of LlLIM1 recombinant proteins to F-actin. In F, 1 mg mL^{-1} commercial F-actin, bovine serum albumin (BSA), and the recombinant proteins indicated were added to the binding solution and centrifuged at 100,000*g* for 45 min. Subsequently, equal amounts of pellets (P) and supernatants (S) were analyzed by SDS-PAGE and Coomassie Blue staining. Only F-actin, not the remaining soluble proteins, was precipitated after high-speed centrifugation. Various amounts (0–48 μM) of LlLIM1 (G and H) and 48 μM BSA (F) were incubated with 4 μM F-actin for 1 h, then centrifuged at 100,000*g* (G) or 12,500*g* (H) for 45 min and analyzed by SDS-PAGE. Equal amounts of pellets (P) and supernatants (S) were analyzed by SDS-PAGE and Coomassie Blue staining.

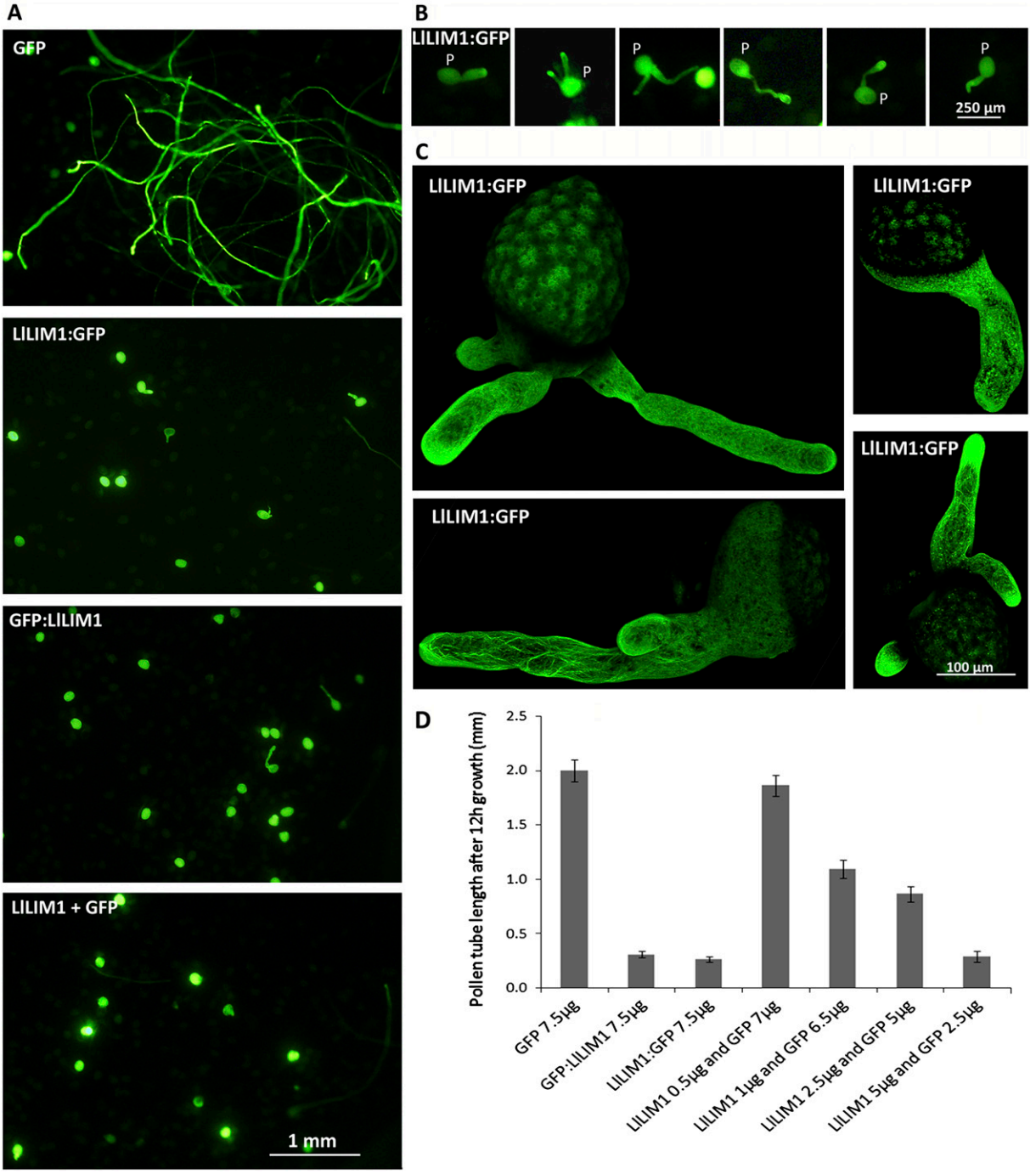

Figure 3. Overexpression of LlLIM1 impaired pollen germination, tube growth, and pollen tube morphology. A and B, Lily pollen grains (P) bombarded with 7.5 μg of GFP-expressing plasmids, LlLIM1:GFP, GFP:LlLIM1, or cobombarded with 2.5 μg of GFP-expressing plasmid and 5 μg of LlLIM1-expressing plasmid were cultured in media for 12 h and observed by epifluorescence microscopy with a GFP filter. C, Projective images of elongating pollen tubes showed multiple pollen tubes emerging from a single pollen grain. Z-serial sections used to assemble the projective images were recorded and edited by fluorescent laser scanning confocal microscopy and an application program. D, Analysis of pollen tube lengths of pollen bombarded with 7.5 μg of the individual plasmids indicated or various combinations of LlLIM1- and GFP-expressing plasmids, but 2.5 μg of GFP-expressing plasmids was used as the minimal amount of transformation marker. A representative example from three independent data sets is shown: control pollen tubes overexpressing GFP showed normal morphology and average length (2.00 $\pm$ 0.10 mm), but the mean length of pollen tubes was reduced with increasing amounts of LlLIM1, such as bombardment with 7.5 μg of LlLIM1:GFP (0.31 $\pm$ 0.03 mm) or GFP:LlLIM1 plasmids (0.27 $\pm$ 0.02 mm) or cobombardment with 5 μg of LlLIM1 and 2.5 μg of GFP plasmids (0.3 $\pm$ 0.05 mm). Error bars indicate 95% confidence intervals (n = 60–80).

examined, only LlLIM1ΔNt:GFP, LlLIM1ΔCt:GFP, and LlLIM1ΔZf4:GFP (Supplemental Fig. S2B) showed F-actin-binding activities in the shank region similar to that of full-length LlLIM1 and LlLIM1N:GFP but not LlLIM1C:GFP, which exhibited weaker affinity to F-actin. A similar observation was confirmed by projecting serial Z-sectioned images under low magnification of individually deleted LlLIM1 constructs (Supplemental Fig. S3). Comparisons of LlLIM1ΔNt:GFP with LlLIM1ΔZf1:GFP and LlLIM1ΔZf4:GFP with LlLIM1ΔLIM2:GFP not only indicated that the integrity of LIM1 domains is critical for the F-actin-binding activity of LlLIM1 but also suggested that both intact LIM domains were required for full F-actin-binding activity of LlLIM1. The purified recombinant 6×His-tagged LlLIM1N and LlLIM1C were further used to verify their F-actin-binding capabilities by cosedimentation assay. Compared with LlLIM1 (Fig. 2G), which started to be coprecipitated with F-actin at 2 μM, LlLIM1N showed weaker binding to F-actin, but LlLIM1C was even weaker than LlLIM1N (Supplemental Fig. S4, A and B). Only full-length LlLIM1 and LlLIM1N but not LlLIM1C showed F-actin bundling (Supplemental Fig. S4, C and D). Both LIM domains interact directly with F-actin, but the higher affinity to F-actin of LlLIM1N than LlLIM1C explains its better F-actin bundling and in vivo F-actin labeling. Similar characteristics of the tandem LIM domains were found in tobacco WLIM1 (Thomas et al., 2007).

To clarify the relation between the F-actin-binding property of LlLIM1 and its effect on pollen tube growth, plasmids expressing different deletions of LlLIM1 (5 μg) were cobombarded with GFP-expressing plasmid (2.5 μg) into pollen, and the tube length was measured 12 h later. As shown in Supplemental Figure S2C, among these variants, only LlLIM1ΔNt, LlLIM1ΔCt, and LlLIM1ΔZf4 severely impaired tube growth, as did overexpression of LlLIM1. These results provide another supporting association between the effect of impaired tube growth and the binding affinity of LlLIM1 to F-actin.

Overexpression of LlLIM1 Increased Resistance to LatB in Pollen Germination by Protecting F-Actin against Depolymerization

Since LatB significantly prohibited pollen germination and tube growth by depolymerizing F-actin (Gibbon et al., 1999; Chen et al., 2007) and LlLIM1 bound tightly to F-actin (Fig. 2), we speculated that overexpressed LlLIM1 might protect F-actin against LatB-mediated depolymerization. As shown in Supplemental Figure S5A, control pollen overexpressing cyan fluorescent protein (CFP) showed normal germination and tube growth in the control medium containing 30 nM dimethyl sulfoxide (DMSO) but not in 10 nM or higher concentrations of LatB-containing culture media. However, pollen grains overexpressing LlLIM1 even germinated and grew better in 10 nM LatB-containing medium compared with medium containing 30 nM DMSO. In 20 nM LatB-containing medium, only intact LlLIM1-overexpressing pollen tubes were able to elongate or germinate. For individual LIM domains, only LlLIM1N-overexpressed pollen tubes could germinate and grow in lower (10 nM) concentrations of LatB-containing culture media. This observation confirmed the higher affinity to F-actin of LlLIM1N than LlLIM1C in F-actin bundling and in vivo F-actin labeling shown above.

The property of LlLIM1 in F-actin in protecting against LatB-mediated depolymerization was further revealed by cosedimentation assay. Most of the commercial F-actin incubated in 192 nM DMSO (the control) was precipitated by 100,000*g* centrifugation (lane 1 in Supplemental Fig. S5B), but 192 nM LatB efficiently depolymerized F-actin and significantly increased depolymerized F-actin in the supernatant fraction after centrifugation (lane 2 in Supplemental Fig. S5B). For LlLIM1, 4 μM recombinant proteins started to protect against depolymerization by 192 nM LatB and prevent F-actin accumulation in the supernatant fraction; and 32 μM LlLIM1 almost satisfactorily protected F-actin against depolymerization by LatB (Supplemental Fig. S5B). Thus, LlLIM1 tightly associated with and protected actin filaments under both in vivo and in vitro conditions. However, neither LlLIM1N nor LlLIM1C showed equivalent protection of F-actin against LatB depolymerization (Supplemental Fig. S5, C and D), probably because of their weaker F-actin-binding affinity than full-length LlLIM1 (Supplemental Figs. S2 and S4).

Overexpressed LlLIM1 Induced Novel Asterisk-Shaped Actin Aggregates and Disturbed Vesicle Trafficking and Oscillatory Pollen Tube Growth

We have demonstrated LlLIM1 functioning as an ABP to enhance F-actin assembly (Fig. 2) and conferring resistance against the LatB-induced depolymerization of F-actin (Supplemental Fig. S5). The tight association of overexpressed LlLIM1 and F-actin may disturb the actin dynamics in the apical and subapical regions to inhibit pollen tube elongation. To test this hypothesis, we used 5 μg of LlLIM1:GFP or GFP (control) to examine their effects on F-actin dynamics in the elongating pollen tube. FM4-64 was used to track the processes of endomembrane trafficking, because FM4-64 is incorporated into the plasma membrane, internalized by endocytosis, and transported to the endosome or recycled back to the plasma membrane (Helling et al., 2006). In growing pollen tubes, FM4-64-labeled vesicles show an inverted cone shape in the clear zone of the tip region enriched with numerous endocytic and exocytic vesicles (Parton et al., 2001). Time-lapse confocal images of pollen tubes expressing GFP showed normal growth (with 0.06–0.15 $\mu m\ s^{-1}$ growth rate), and FM4-64-stained vesicles with an inverted cone shape accumulated in the clear zone of the tube tip (Supplemental Fig. S6A; Supplemental Movie S1). Nevertheless, LlLIM1:GFP-overexpressed pollen tubes showed greatly reduced

typical growth (with a slow growth rate of $<0.05\ \mu m\ s^{-1}$) and contained much fine, short, and dynamic F-actin in the tip region (Supplemental Fig. S6B; Supplemental Movie 2). In the meantime, FM4-64-stained vesicles started to aggregate in the subapical zone and lost the typical inverted cone-shaped vesicles. For pollen tubes without visible oscillatory growth, unusual asterisk-shaped F-actin bundles intensively labeled with LlLIM1:GFP appeared in the subapical zone simultaneously and intensively colocalized with FM4-64-labeled vesicles (Supplemental Fig. S6C; Supplemental Movie 3). Interestingly, the pollen tubes with slowed and stopped growth were still alive, as evidenced by their normal cytoplasmic streaming (as revealed by the organelle movement in the differential interference contrast images in Supplemental Fig. S6, B and C). These phenomena suggest that excess LlLIM1 overstabilizes and probably enhances F-actin bundle formation to impair actin dynamics in the tip region and eventually results in retarded normal tube elongation.

Overexpressing LlLIM1 Induced the Mislocalization of Several Signaling Molecules and the Golgi Apparatus to Disturb Vesicle Trafficking in the Clear Zone of the Elongating Pollen Tube

Helling et al. (2006) and Dowd et al. (2006) suggested that the targeting of the PLC-mediated signaling pathway is mediated by endomembrane trafficking in the pollen tube. Overexpression of LlLIM1 in pollen tubes disturbed the trafficking of FM 4-64-stained vesicles in the clear zone, which may also affect the targeting of these membrane-associated signal molecules in the tip region. Next, we examined the distribution of PLC-related signaling molecules such as PIP2/PLC and DAG, as well as the Golgi apparatus, in pollen tubes overexpressing LlLIM1. PIP2 accumulates at the extreme apical plasma membrane of rapidly growing pollen tubes of petunia (*Petunia hybrida*; GFP-tagged N terminus of PetPLC1; Dowd et al., 2006) and tobacco (yellow fluorescent protein [YFP]-tagged PH domain of human PLCδ1; Helling et al., 2006), but DAG recycles from the apical flank membrane to the apical membrane in elongating pollen tubes (Helling et al., 2006), as visualized by fluorescent protein-tagged Cys-1 (Oancea et al., 1998). Therefore, we used fluorescent protein-tagged PH and Cys-1 domains to track the distribution of PIP2/PLC and DAG in CFP- (control) or LlLIM1-overexpressed pollen tubes.

As shown in Supplemental Figure S7, in YFP:PH- and CFP-cobombarded lily pollen tubes, the typical apical membrane-localized PIP2/PLC was revealed (top panel), as was reported previously (Dowd et al., 2006; Helling et al., 2006). However, YFP:PH- and LlLIM1-cotransformed pollen tubes with slow growth exhibited a faint YFP:PH signal in the apical plasma membrane (middle panel), but for growth-arrested pollen tubes, no YFP:PH signal was detected (bottom panel). These extraordinary localization patterns differ greatly from the results of early studies showing apical membrane-localized PIP2/PLC, persisting even with pollen tube growth stopped by normal culture conditions (Dowd et al., 2006) and/or 50 nM LatB treatment (Helling et al., 2006), in which the actin dynamics were less affected in both conditions. The above results highlight that properly regulated actin dynamics are critical to precisely locate and relocate PIP2 along the apical plasma membrane during pollen tube elongation. DAG, in the control pollen tubes with coexpressed CFP and CYS1:GFP, mainly localized along the plasma membrane of the apical tip and was well colocalized with FM4-64 (Fig. 4A), as was found in tobacco pollen tubes (Helling et al., 2006). Nevertheless, for pollen tubes overexpressing LlLIM1, in slowly growing tubes, both plasma membrane-localized DAG and FM4-64 started to accumulate in the cytoplasm (Fig. 4B, left and middle panels) and occasionally colocalized with aggregated FM4-64-stained vesicles near the plasma membrane of the clear zone (Fig. 4B, right panel). On the contrary, as the pollen tube stopped growing, many FM4-64- and CYS1:GFP-labeled vesicles aggregated in the subapical center (Fig. 4C), but the plasma membrane-associated CYS1:GFP and FM4-64 vesicles increased significantly in number compared with in the slowly growing tube. For FM4-64, a significant amount of FM4-64-labeled vesicles near and/or associated with the plasma membrane were found in slowly growing pollen tubes, but most FM4-64 molecules were trapped in the plasma membrane in tubes that had stopped growing (Fig. 4, B versus C).

In the elongating pollen tube, membrane and cell wall materials are rapidly exported and targeted to the tip region through TGN-derived secretory vesicles in the clear zone (Picton and Steer, 1983). Golgi mobility largely depends on actin dynamics; therefore, we monitored the distribution of the Golgi apparatus in LlLIM1-overexpressing pollen tubes by the CFP-tagged Golgi marker NAG (for N terminus of Arabidopsis *N*-acetylglucosaminyl transferase I; Dixit and Cyr, 2002). Coexpression of GFP and NAG:CFP localized dynamically, and rapidly moving Golgi apparatuses in the cytoplasm were shown as numerous bright clouds in the tip region (Fig. 5A), as was observed in the petunia pollen tube (Dowd et al., 2006). In slowly growing pollen tubes with overexpressed LlLIM1:GFP, the dynamic movement of the Golgi apparatus slowed down and aggregated as bright speckles in the subapical regions, where they were enriched with LlLIM1-decorated F-actin cables (Fig. 5B). In pollen tubes that stopped growing, Golgi bodies showed extensive aggregation in the subapex around the asterisk-shaped actin bundles intensively decorated by LlLIM1:GFP (Fig. 5C). All of these results highlight that a functional actin dynamic network is essential for proper endomembrane trafficking and signal molecules targeting in the elongating pollen tube. Overexpression of LlLIM1 will enhance actin bundle formation to lose F-actin network plasticity,

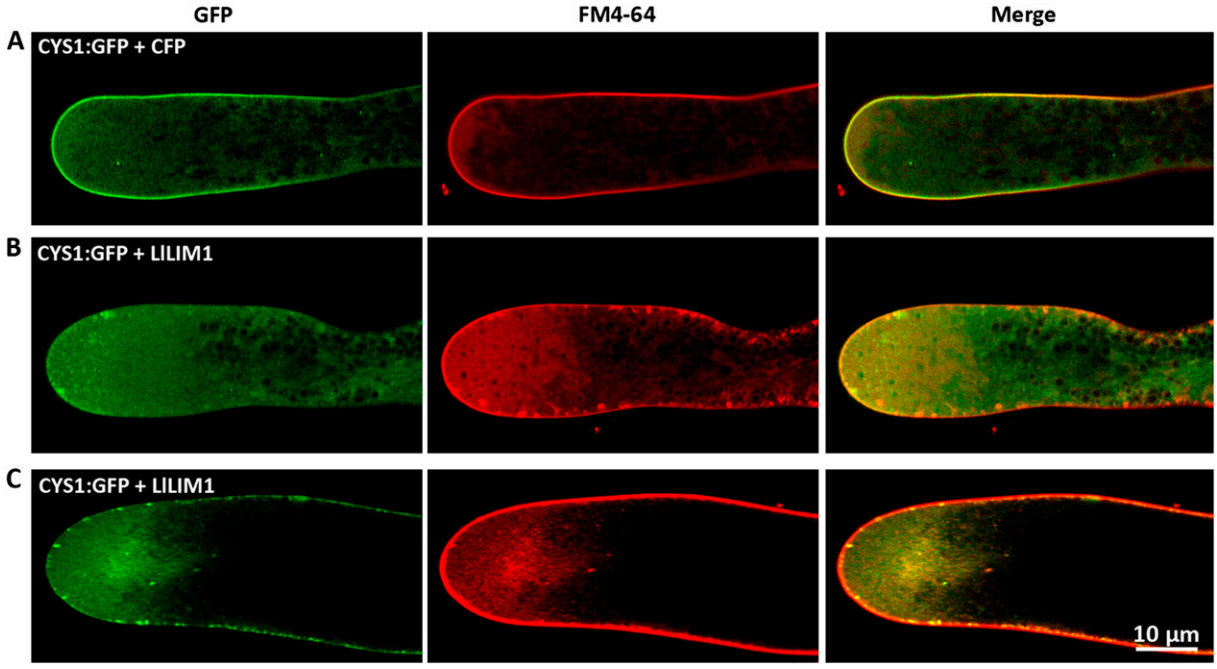

Figure 4. LlLIM1 overexpression caused the mislocalization of signal molecules involved in the PLC signaling pathway in the clear zone of elongating pollen tubes. The images show the typical (A) and missed (B and C) subcellular localization of the fluorescent DAG marker, CYS1:GFP, in CFP-co-overexpressed (A) or LlLIM1-co-overexpressed (B and C) pollen tubes stained with FM4-64 to show the distribution of secreted/endocytic vesicles. B and C represent pollen tubes showing slow and stopped growth, respectively. In all experiments, pollen grains were cobombarded with 2.5 μg of expressing plasmid of the indicated florescent markers and 5 μg of expressing plasmid of CFP or LlLIM1, cultured in germination medium for 6 h, and then confocal images were recorded with the proper fluorescent channels. Images were obtained from the central section of pollen tubes lying flat on the cover-slide surface and represent typical examples from at least 10 similar images collected from at least three independent experiments.

which will disturb all of the above events to result in arrested pollen tube growth.

pH and Ca^{2+} Simultaneously Regulate the Binding Ability of LlLIM1 to F-Actin

To investigate the possible mechanism of LlLIM1 in controlling F-actin flexibility and dynamics and pollen tube oscillatory growth, we applied a moderate dosage of LlLIM1:GFP (3 μg of plasmids), and some transformed pollen tubes showed the periodic fluctuation of the asterisk-shaped F-actin structure in the subapical zone (Fig. 6A; Supplemental Movie S4). The velocity of pollen tube growth was significantly reduced during the concurrent appearance of these asterisk-shaped aggregates labeled with LlLIM1:GFP. The asterisk-shaped actin aggregates appeared during the slow growth phase and disappeared just prior to the resumption of pollen tube growth (Fig. 6B, asterisks). These observations raise the possibility that some important inherent oscillators may regulate the binding affinity of LlLIM1 to F-actin and the associated vesicle trafficking inside the pollen tube between fast and slow growth phases.

pH and $[Ca^{2+}]_c$ showing intracellular gradient oscillation in the clear zone are well-known central oscillators in regulating pollen oscillatory growth (Feijó et al., 1999). Because pH, Ca^{2+}, and LlLIM1-induced asterisk-shaped actin aggregates show periodic fluctuation in the elongating pollen tube, the F-actin-binding activity of LlLIM1 may be modulated by either pH or Ca^{2+} or both simultaneously. To test this hypothesis, we performed F-actin-mediated LlLIM1 sedimentation assays under different pH and Ca^{2+} incubation conditions. To precisely evaluate the efficiency of LlLIM1 and F-actin coprecipitation, we used the minimal amount of LlLIM1, 2 μM, previously showing binding affinity to F-actin (Fig. 2G). First, we incubated 2 μM LlLIM1 and 2 μM commercial F-actin mixtures under nine different binding buffers with different pH buffered by MES or Tris base (pH 6.25, 6.5, 6.75, and 7 in MES buffer; pH 7, 7.25, 7.5, 7.75, and 8 in Tris buffer) to mimic the internal pH range in the elongating pollen tube. After 1 h of incubation, the mixtures were centrifuged at 100,000*g*, and the pellets and supernatants were fractionated by SDS-PAGE and stained by Coomassie Blue. No mixtures showed enhanced binding activity of LlLIM1 to F-actin (Fig. 7A, top panel) or affected the solubility of LLIM1 (Fig. 7A, bottom panel). Since the commercial F-actin was stored in the buffer containing 0.2 mM $CaCl_2$, we speculated that this high $[Ca^{2+}]$ might interfere with LlLIM1 binding to F-actin. We reduced the $[Ca^{2+}]$ by titrating the commercial F-actin with 4 mM EGTA. Surprisingly, with reduced $[Ca^{2+}]$ to about 330 nM Ca^{2+}, the binding efficiency of LlLIM1 to F-actin was

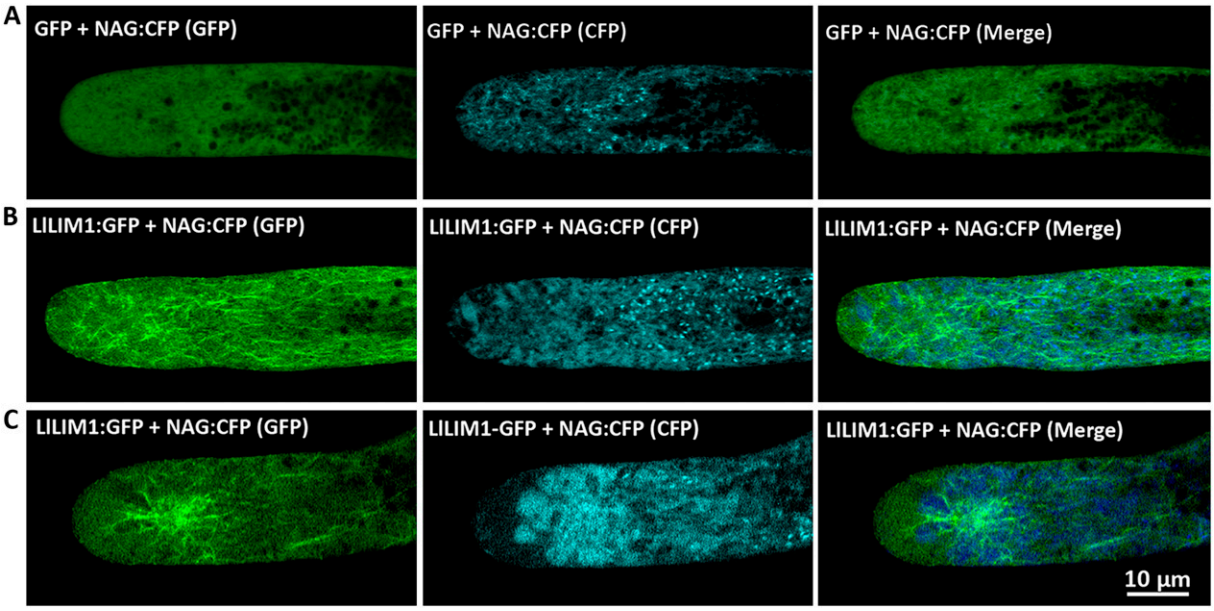

Figure 5. LlLIM1 overexpression-aggregated Golgi apparatus at the subapical zone of the elongating pollen tube. The subcellular localization of the fluorescent Golgi apparatus was revealed by the marker NAG:CFP in GFP-co-overexpressed (A; control) or LlLIM1:GFP-co-overexpressed (B and C) pollen tubes, which represent pollen tubes showing slow or stopped growth, respectively. In all experiments, pollen grains were cobombarded with 2.5 μg of expressing plasmid of the indicated fluorescent markers and 5 μg of expressing plasmid of GFP or LlLIM1:GFP, cultured in germination medium for 6 h, and then confocal images were recorded with the proper fluorescent channels indicated at the top of the panels. Images were obtained from the central section of pollen tubes lying flat on the cover-slide surface and represent typical examples from at least 10 similar images collected from at least three independent experiments.

significantly enhanced under low pH buffer conditions, with the highest binding capacity being pH 6.25 (Fig. 7B). This result pointed out the critical role of $[Ca^{2+}]$ and pH in regulating the affinity of LlLIM1 to F-actin. Then, to optimize the $[Ca^{2+}]$ for higher F-actin-binding capacity, LlLIM1 and F-actin mixtures were incubated in the buffer pretreated with various amounts of EGTA under pH 6.25, then they underwent cosedimentation assay analysis. The estimated concentrations of free Ca^{2+} in these buffers containing different amounts of EGTA ranged from 170 nM to 38 μM, as calculated by the EqCal program (detailed in "Materials and Methods"). As shown in Figure 7C, the F-actin-binding activity of LlLIM1 was increased, starting at 3 mM EGTA (approximately 440 nM Ca^{2+}) and peaking at 8 mM EGTA (approximately 170 nM Ca^{2+}). All of these results reveal that LlLIM1-F-actin-binding activity can be enhanced by acidic and low $[Ca^{2+}]$ circumstances; they also provide a reasonable explanation for the asterisk-shaped actin structures showing intermittent occurrence related to pollen tube oscillatory growth. As the pollen tube enters a slow growth phase, the acidic and low-$[Ca^{2+}]_c$ conditions in the tip region (Holdaway-Clarke et al., 1997; Lovy-Wheeler et al., 2006) promote the binding affinity of overexpressed LlLIM1 to F-actin to result in the asterisk-shaped actin aggregates.

We also examined the F-actin-binding affinity of truncated LlIM1N and LlLIM1C recombinant proteins under the above conditions to determine which domain was involved in perceiving the change in pH and $[Ca^{2+}]$ to control the F-actin-binding property. From previous cosedimentation results (Supplemental Fig. S4, A and B), we applied 6 and 28 μM LlLIM1N and LlLIM1C recombinant proteins, respectively. Similar to LlLIM1, LlLIM1N (Fig. 7D) and LlLIM1C (Fig. 7G) showed no F-actin-binding activity under various pH levels but, rather, did so under high $[Ca^{2+}]$ conditions. However, under 4 mM EGTA with low pH (pH 6.25, 6.5, and 6.75; Fig. 7, E and H) and pH 6.25 with different amounts of EGTA-treated buffering conditions (Fig. 7, F and I), only LlLIM1N but not LlLIM1C showed gradually increasing F-actin-binding efficiency with decreased $[Ca^{2+}]$. Thus, the first LIM domain probably contributes the pH- and $[Ca^{2+}]$-sensing property of LlLIM1. In conclusion, our data indicate that LlLIM1 functions as an ABP, and its regulatory binding activity in controlling actin dynamics and oscillatory growth in the apical domain of the elongating pollen tube is simultaneously mediated by pH and $[Ca^{2+}]_c$ oscillation, probably through its first LIM domain.

DISCUSSION

The elongating pollen tube exhibits highly polarized endomembrane trafficking and growth. The actin cytoskeleton is believed to provide the major driving

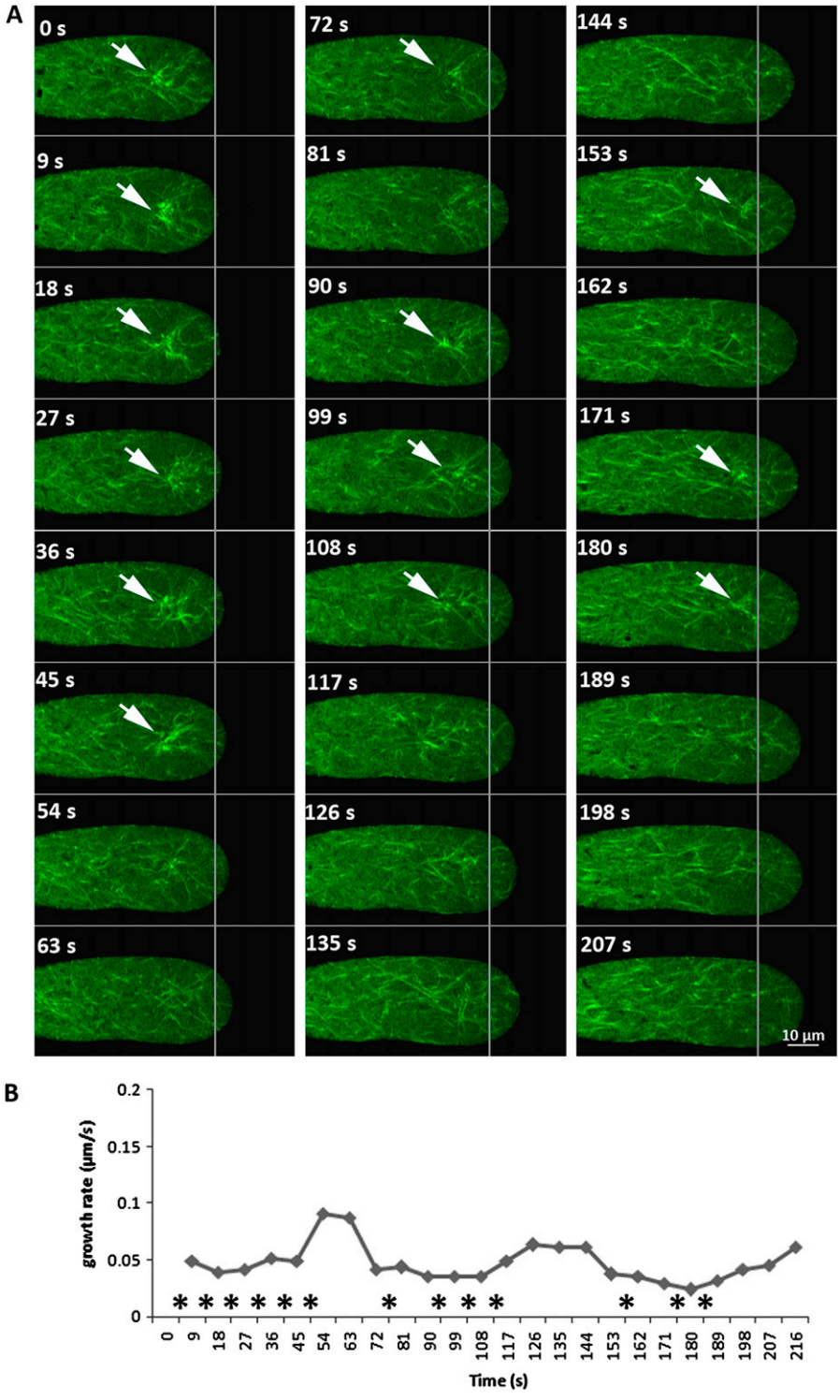

Figure 6. Periodic appearance of asterisk-shaped actin aggregates closely associated with oscillatory growth in pollen tubes moderately expressing LlLIM1:GFP. A, Serial images from one typical pollen tube bombarded with 3 μg of LlLIM1:GFP-expressing plasmids showed the oscillatory appearance of asterisk-shaped actin aggregates and growth after culture in germination medium for 6 h. Consecutive confocal time-lapse images were recorded at 9-s intervals with the GFP channels; white lines represent the initial length (at 0 s) of the pollen tube. Arrows indicate the subapical localization of asterisk-shaped actin aggregates. In all cases, the central section of pollen tubes lying flat on the cover-slide surface are shown and represent at least three similar serial images collected from at least two independent experiments. B, Diagram of the curve showing the continuing growth rate of the pollen tube obtained from A; asterisks indicate the time points around fast growth peaks when asterisk-shaped actin aggregates appeared. [See online article for color version of this figure.]

force for these processes, but the actin dynamics and organization regulated by ABPs and interaction with other oscillators to coordinate these processes are not fully understood. In this study, we demonstrated that LlLIM1-mediated actin binding and bundling activities participated in the regulation of actin dynamics and configuration to control endomembrane organization and pollen tube elongation. In vivo and in vitro functional assays revealed that both LIM domains were required for LlLIM1-promoted F-actin cable formation and protected against F-actin depolymerization by LatB, as its counterpart NtWLIM1 does in tobacco BY2 cells (Thomas et al., 2006, 2007). In addition, overexpressed LlLIM1 significantly disturbed the

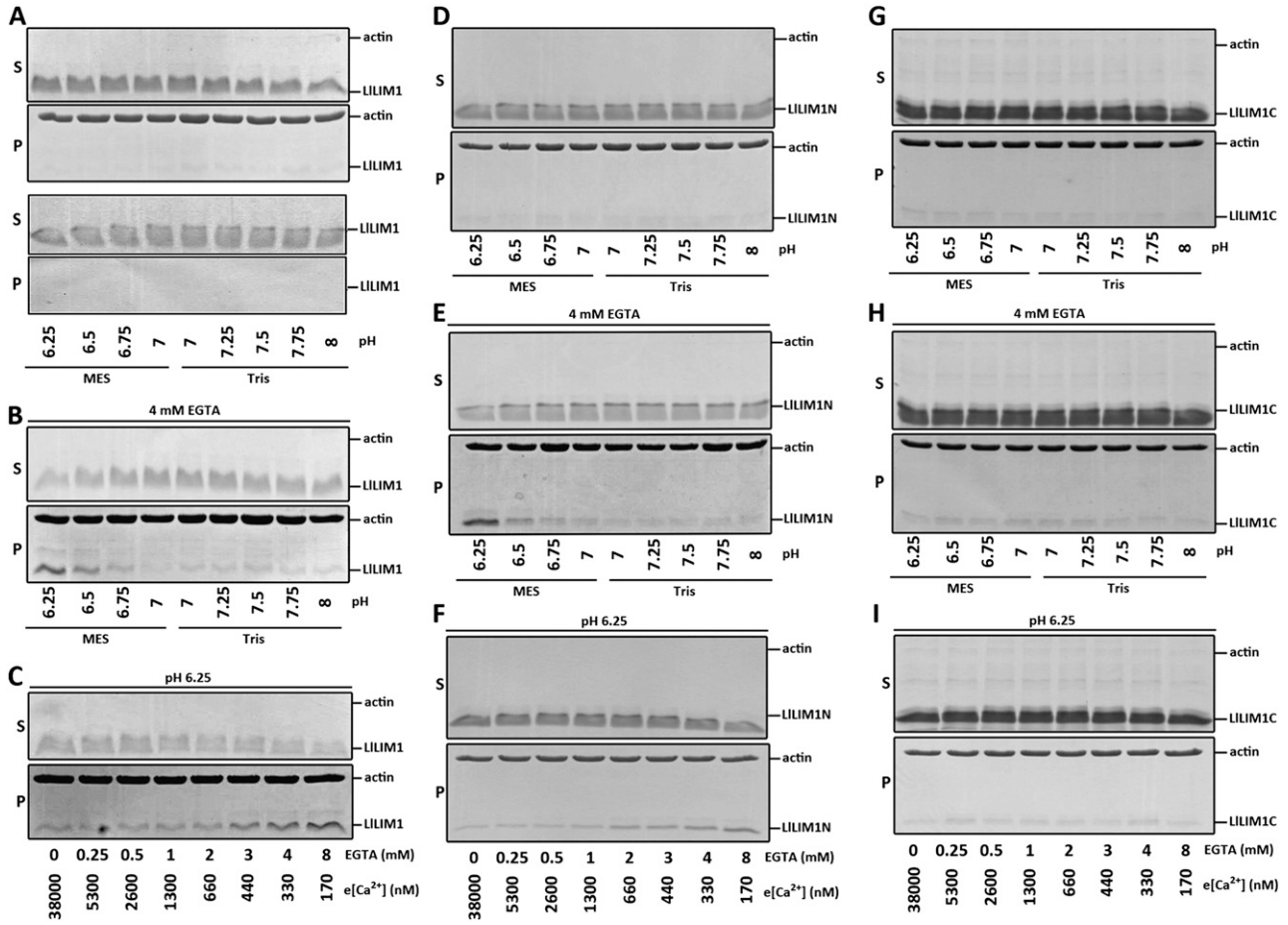

Figure 7. In vitro high-speed cosedimentation assays revealed that $[H^+]$ and $[Ca^{2+}]$ simultaneously regulated the F-actin affinity of full-length and the N-terminal half of LlLIM1. High-speed (100,000*g*) F-actin in vitro cosedimentation assay samples were collected from reaction buffers containing 4 μM F-actin and 2 μM LlLIM1 (A–C), 6 μM LlLIM1N (D–F), or 28 μM LlLIM1C (G–I) under different pH conditions (pH 6.25–7, MES buffer; pH 7–8, Tris buffer) without (A, D, and G) or with (B, E, and H) 4 mM EGTA. C, F, and I were samples from reaction buffers containing 4 μM F-actin and 2 μM LlLIM1, 6 μM LlLIM1N, or 28 μM LlLIM1C under pH 6.25 conditions and in the presence of different amounts of EGTA (0–8 mM) used for cosedimentation assays with the estimated $[Ca^{2+}]$ indicated. In all experiments, after 1 h of incubation, the samples were centrifuged at 100,000*g* for 45 min, and the resulting pellet (P) and supernatant (S) fractions were analyzed by SDS-PAGE and Coomassie Blue staining. e$[Ca^{2+}]$, Free Ca^{2+}.

F-actin dynamics by forming subapical F-actin aggregates to impair normal targeting of signaling molecules (PIP2, PLC, and DAG) and disturbed the endomembrane trafficking (Golgi apparatus and DAG-labeled vesicles for exocytosis and endocytosis, respectively) to retard pollen tube elongation. Importantly, in vitro cosedimentation results showed that the F-actin-binding affinity of LlLIM1 was concurrently regulated by pH and Ca^{2+}, the highest binding activity being pH 6.25 and 170 nM Ca^{2+}. All of these results suggest that LlLIM1 functions as part of the central oscillator mechanism, with pH and Ca^{2+}, to regulate and/or protect F-actin dynamics during pollen tube oscillatory growth. A loss-of-function approach, overexpression of antisense *pZM13*::*LlLIM1*, was used to investigate the possible function of LlLIM1, but no obvious phenotype or growth defect was found in transformed pollen tubes (data not shown). This result may be due to gene redundancy: genome-wide analyses have revealed several pollen-specific *LIM* families present in Arabidopsis, tobacco, rice, and *Populus trichocarpa* pollen (Arnaud et al., 2007). Our use of RT-PCR and promoter-GUS activity transgenic assays revealed *AtWLIM1* to be highly expressed in vegetative tissues and anther/pollen, but the other two Arabidopsis *LIM*s (At1g01780 and At3g61230) exhibited pollen-specific expression patterns (H.-J. Wang and G.-Y. Jauh, unpublished data).

LlLIM1 Functions as a Novel ABP in Stabilizing/Promoting F-Actin Bundling to Control Endomembrane Trafficking and Signal Molecule Targeting in the Elongating Pollen Tube

Most LIM proteins (LIMs) function as a modular protein-binding interface participating in an array of biological processes through binding to specific target

proteins as adaptors, competitors, autoinhibitors, or localizers (Schmeichel and Beckerle, 1997). In animals, LIMs function as transcriptional factors in the nucleus (e.g. LMO2 [Wadman et al., 1997] and LHX [Thaler et al., 2002]) or as actin association proteins in the cytoplasm (e.g. LIM kinase [Arber et al., 1998] and EPLIN [Maul et al., 2003]) or with dual functions in both compartments (e.g. the CRP family [Schmeichel and Beckerle, 1997; Grubinger and Gimona, 2004; Tran et al., 2005]). In flowering plants, several CRP-related LIM orthologs have been found in Arabidopsis, rice (Arnaud et al., 2007), tobacco (Eliasson et al., 2000), sunflower (Baltz et al., 1992), and lily pollen (this study). Although a few plant LIMs showed nuclear localization, such as NtWLIM1 (Thomas et al., 2006), LlLIM1 was seldom found in the vegetative nucleus of the pollen tube (data not shown). Analysis of the tandem zinc finger modules in both LIM domains of all plant LIMs revealed that some inherited functional difference may exist between the two LIM domains of plant LIMs. The first LIM domain showed a conserved sequence similar to the animal LIM sequence (Schmeichel and Beckerle, 1997). However, in the second LIM domain, the sequence of the second zinc finger motif is C-X4-C-X15-C-X2-H instead of the typical C-X2-C-X17-C-X2-H found in most animal LIMs. Serial experimental results revealed that the two LIM domains of LlLIM1 showed quantitative differences in affinity to F-actin in vivo and in vitro (Supplemental Figs. S2 and S4), resistance to LatB treatment (Supplemental Fig. S5), and sensitivity to pH and calcium-regulated actin-binding affinity (Fig. 7). Nevertheless, the molecular mechanism and the critical amino acid residues in the LIM domain involved in this discrimination remain largely unexplored.

The assembly of higher-order F-actin bundles mediated by actin bundlers is important for many cellular events, such as muscle contractibility, cytoplasmic streaming, organelle migration, and endomembrane trafficking (Hussey et al., 2006; Thomas et al., 2006). Plants have at least three classes of F-actin bundlers: villins, fimbrins, and elongation factor-1α. Villin and fimbrin are well-characterized F-actin-bundling factors and possess resistance to ADF/cofilin- and profilin-induced actin depolymerization, respectively (Kovar et al., 2000; Huang et al., 2005). Villin localizes to actin cables in root hair (Tominaga et al., 2000) and the lily pollen tube, whereas two villins, P-115-ABP and P-135-ABP, bundle actin filaments under a basal level of [Ca^{2+}], but their bundling activities are prohibited in the presence of high [Ca^{2+}] and calmodulin (Yokota et al., 2003, 2005). However, the activity of Arabidopsis VILLIN1 was insensitive to [Ca^{2+}] (Kovar et al., 2000; Huang et al., 2005). The regulation of fimbrin binding activity to F-actin is still unclear, but its activity is [Ca^{2+}] insensitive (Kovar et al., 2000). Elongation factor-1α is a dual-function protein with aminoacyl tRNA binding as well as actin-binding and -bundling activities (Gungabissoon et al., 2001). In this study, we demonstrated that pH and [Ca^{2+}] can simultaneously regulate the F-actin binding of LlLIM1. The above results suggest that these proteins probably have different regulatory mechanisms for F-actin affinity to accomplish their physiological regulation in F-actin dynamics. Overexpression of LlLIM1 retarded pollen tube growth in a dose-dependent manner (Fig. 3), probably because of slowing down and disordered pollen tube oscillatory growth (Fig. 6B). In addition, high dosage of overexpressed LlLIM1 caused pleiotropic tip morphology, including abnormal tip, slightly swollen tip, and even multiple tubes emerging out of a single pollen grain (Fig. 3, B and C), which suggests a sequential instead of a simultaneous developmental process of this unique phenotype. When the first-emerged pollen tube stopped growing with LlLIM1 overstabilized apical actin filaments, the living pollen still had vitality to protrude a second tube tip from the basal region of the existing pollen tube; however, the continuous growth of this tube was inhibited again by overexpressed LlLIM1. This phenomenon is similar to the effect of jasplakinolide, a sponge cyclodepsipeptide, which stabilized and promoted the polymerization of F-actin, significantly reduced pollen germination, decreased growth velocity and cytoplasmic streaming in the shank of the tube, and induced the formation of a torpedo-shaped domain in the swollen apex (Cardenas et al., 2005). In addition, low-dosage LatB had no effect on cytoplasmic streaming and actin bundling in the shank of pollen tubes but significantly ceased tip growth and disrupted subapical actin dynamics (Gibbon et al., 1999; Vidali and Hepler, 2001). All of these findings raise the possibility that functional but sensitive apical actin dynamics plays a more important role in the elongation than the emergence of a pollen tube. Further examination is required to verify this idea.

Cell growth and maintenance need massive exocytic and endocytic vesicles to transport and recycle membrane and wall/extracellular matrix materials (Cheung and Wu, 2008). An estimated 80% or more of the membrane fusing with the tip is recycled during pollen tube growth (Picton and Steer, 1983). BFA, a fungal macrocyclic lactone, significantly prohibits membrane trafficking via the release or inactivation of Golgi coat proteins. In plant cells, BFA induced the formation of large clusters of fused secretory vesicles, called BFA compartments, which are primarily composed of TGN vesicles (Šamaj et al., 2004, 2005). In the pollen tube, BFA treatment caused retrograde transport of the FM4-64-tagged membrane from the tube tip back to a distinct subapical BFA-induced membrane aggregation (BIA) compartment (Parton et al., 2001, 2003), where a basket-shaped aggregate of actin filaments formed (Hörmanseder et al., 2005). The basket-shaped actin aggregates colocalized with the BIA compartment, and retrograde transport of FM4-64-labeled membrane was significantly disturbed by the cytoskeleton-disturbing drugs, which suggests that the integrity of BIA and associated movement were actin dependent. Similar aggregation of FM4-64-labeled vesicles, coupled with LlLIM1:GFP-labeled

asterisk-shaped F-actin aggregates, was found at the subapical region of pollen tubes (Fig. 4; Supplemental Fig. S6). Whether this F-actin structure is the same as the subapical basket-shaped F-actin aggregates observed by Hörmanseder et al. (2005) in BFA-treated cells remains to be determined. The formation of unique subapical asterisk/basket-shaped F-actin aggregates induced by LlLIM1 overexpression provides a unique tool to investigate the dynamic compartmental organization in the pollen tube tip. In addition to the FM4-64-labeled vesicles, many NAG:CFP-stained Golgi networks as well as the DAG molecules are colocalized with asterisk-shaped F-actin aggregates in pollen tube tip (Fig. 5). Dowd et al. (2006) showed persistent apical localization of PLC in the spontaneous nongrowing petunia pollen tube. Our overexpression of LlLIM1 also caused mislocalization of PLC-related signal molecules (Fig. 4; Supplemental Fig. S7). Overexpressed LlLIM1 might disturb the F-actin-mediated exocytosis to reduce the accumulation of PIP2 in the apical membrane by either mislocalizing a putative membrane-localized PIP kinase or membrane-localized PLC continuously depleting the preexisting PIP2, or both. DAG can be internalized from the apical flanking region and retrotransported to the apical membrane in the elongating pollen tube (Helling et al., 2006). Tobacco pollen tubes overexpressing an endosomal marker FYVE domain caused the formation of enlarged endocytic compartments, which trapped DAG (Helling et al., 2006). This idea was supported by LlLIM1 overexpression impairing the recycling and retargeting of DAG to accumulate in cytosolic endomembrane compartments, where it colocalized with FM4-64-labeled vesicles (Fig. 4C), as was found in BFA-treated tobacco pollen tubes (Helling et al., 2006). In pollen tubes that had stopped growing, DAGs produced by the apical membrane could have mislocalized PLC, but the bulk membrane translocation from the extreme pollen tube apex back to subapical BIA was completely impaired by LlLIM1-stabilized F-actin to trap the DAGs and FM4-64 in the apical membrane. Recently, Dettmer et al. (2006) found that VHA-a1, a subunit of membrane-integral V-ATPase, was preferentially found in the TGN; however, subcellular colocalization of the VHA-a1 and FM4-64 implied that the TGN might function as an early endosomal compartment in plant cells. Therefore, it has been suggested that TGN may represent a dynamic apical compartment integrating exocytosis and endocytosis within typical tip-extending cells (Šamaj et al., 2006). All of these results point to LlLIM1 being involved in apical and subapical actin dynamics, which are critical for polar growth, Golgi network dynamics, and the transport of exocytic and endocytic vesicles in the elongating pollen tube.

Regulation of F-Actin-Binding Activity and Potential Role of LlLIM1 in Regulating Pollen Tube Growth

Time-lapse images of the dynamic change in $[Ca^{2+}]_c$ obtained from fura-2-dextran-loaded lily pollen tubes showed a tip-focused $[Ca^{2+}]_c$ gradient with the shank of the pollen tube of 100 to 500 nM and the extreme apex reaching 1 to 10 μM and oscillating with the same period as oscillatory growth (Holdaway-Clarke et al., 1997). Microinjection of the lily pollen tube with the pH-sensitive dye bis-carboxyethyl carboxyfluorescein dextran showed an oscillatory pH change in the apical region ranging from 6.8 to 7.5 (Feijó et al., 1999). Recently, Lovy-Wheeler et al. (2006) demonstrated an oscillating pH alteration in the apical domain closely related to pollen tube oscillatory growth: increased pH preceded the fastest growth velocities, whereas decreased pH followed growth. Formation of LlLIM1-induced asterisk-shaped actin aggregates also exhibited oscillatory changes closely correlated to pollen tube growth (Fig. 6). Thus, LlLIM1-mediated F-actin-binding and -bundling activities in the apical domain might be regulated by oscillatory pH and $[Ca^{2+}]$ gradients. Our F-actin cosedimentation assay confirmed this idea by showing that pH and $[Ca^{2+}]$ simultaneously regulated the F-actin-binding activity of recombinant LlLIM1: LlLIM1 possesses higher F-actin-binding capacity under both low $[Ca^{2+}]$ (170 nM) and low pH (pH 6.25) conditions. Although both pH and $[Ca^{2+}]$ regulated the affinity of LlLIM1 to F-actin, pH seemed to play a more critical role than did $[Ca^{2+}]$. As pH increased from 6.25 to 6.75, the affinity of LlLIM1 to F-actin decreased greatly and dropped to the basal level around pH 7.0 (Fig. 7B). Nevertheless, an obvious affinity of LlLIM1 with F-actin was present at pH 6.25 even under high $[Ca^{2+}]$, such as 440 nM (Fig. 7C), which suggests that its activity could be less sensitive to local changes in $[Ca^{2+}]_c$.

On the basis of our results and those in the literature, we hypothesize possible sequential events with the incorporation of pH, Ca^{2+}, and several ABPs, including LlLIM1, in regulating pollen tube oscillatory growth. Since LlLIM1 showed the highest binding affinity to F-actin under low pH and $[Ca^{2+}]_c$, which, present at the shank of the pollen tube during the growth-paused phase, will enhance the binding of LlLIM1 to F-actin to stabilize and/or protect existing F-actin cables from depolymerization by other severing ABPs. Prior to the initiation of the fast growth phase, a putative subapical membrane-localized H^+-ATPase will efflux the H^+ to form a subapical alkaline band (Feijó et al., 1999) to accelerate (1) the dissociation of LlLIM1 from the preexisting F-actin and (2) the association of the alkaline ADF with many short, fine, and fringe actin filaments in the subapex of the pollen tube (Chen et al., 2002; Lovy-Wheeler et al., 2006). ADF-exposed barbed ends in these actin fringes provide the entries for other F-actin polymerization factors (such as formin) to polymerize and prolong actin filaments that will be ready for the travel tracks for subapically accumulated Golgi-derived vesicles rapidly transported to the apical membrane to initiate fast pollen tube extension (Cheung and Wu, 2004, 2008; Lovy-Wheeler et al., 2006). Overexpressed LlLIM1s stabilize the subapical actin network to impair Golgi

network-mediated transport and targeting of membrane and signaling molecules to the tip region. As the fast-growing phase initiates, the influx of proton and calcium driven by the putative apical strength-activated proton and calcium channels increases significantly (Feijó et al., 1999; Dutta and Robinson, 2004) and eventually reduces subcellular pH, but it increases $[Ca^{2+}]_c$ to inactivate alkaline ADF/AIP1 activities (Lovy-Wheeler et al., 2006) as well as to disorganize the apical actin microfilament system by villin (Yokota et al., 2005). Under this high $[Ca^{2+}]_c$ condition at the apical region, the activities of actin polymerization regulated by profilin (Kovar et al., 2000) are greatly reduced; however, fragmentation of F-actin by gelsolin, a Ca^{2+}-dependent actin filament-severing protein identified from pollen, is effectively activated (Fan et al., 2004; Huang et al., 2004). Eventually, locally high $[Ca^{2+}]_c$ in the apical region may destroy formin-built actin microfilaments by the coordinated function of villin/gelsolin and profilin to reduce growth velocities. Reduction of pollen tube growth will slow the influx of proton and calcium by inactivating the corresponding putative strength-activated channels to reduce $[Ca^{2+}]_c$ to the basal level and keep a lower pH level at the shank of the pollen tube. Under the slow growth phase, the lower intracellular pH will play a major role in binding LlLIM1 to F-actin, with less sensitivity to local changes in $[Ca^{2+}]_c$. Because continuous depletion of Ca^{2+} occurred at the shank of the pollen tube, the affinity of LlLIM1 with F-actin will be strengthened to protect the preexisting actin filaments during the growth-pause stage to wait for another cycle of oscillatory growth. Use of an improved cryofixation and immunofluorescent (actin and ADF antibodies) procedure revealed a dense F-actin fringe starting 1 to 5 μm from the apex and spanning 5 to 10 μm along the apical flank in the lily pollen tube (Lovy-Wheeler et al., 2005, 2006). However, a similar actin structure was never observed in the LlLIM1-overexpressed pollen tube. The different localizations of various ABPs are critical for their functions in regulating F-actin dynamics. For example, pH oscillates from 6.8 to 7.5 in the apical region of the elongating pollen tube (Feijó et al., 1999), and the activity of ADF is enhanced in the alkaline band near the apical region to form a fringe actin structure (Allwood et al., 2002; Chen et al., 2002; Lovy-Wheeler et al., 2006). However, LlLIM1 has strong actin affinity under low pH and $[Ca^{2+}]$ conditions, which may protect the nascent actin filament in the subapical region. In addition, Wilsen et al. (2006) used several GFP-tagged ABPs to reveal a diverse pattern of F-actin in transiently transformed living pollen tubes, and none revealed the entire spectrum of the actin network. All of these results highlight the importance of the F-actin/ABP integrity network and dynamics in the apical and subapical regions contributing to the polar cell growth process.

We have shown that overexpression of LlLIM1 in pollen tubes causes subapical aggregation of the Golgi network and FM4-64-stained vesicles (Fig. 5C; Supplemental Fig. S6C), as an early study showed that FM4-64-stained vesicles accumulated in the region 3 to 5 μm back from the apex and oscillated over time during the same time as growth but 5 to 10 s earlier than the oscillatory growth rate (Parton et al., 2001). Therefore, we cannot rule out the possibility that LlLIM1-mediated actin dynamics is probably also involved in regulating the oscillatory targeting of vesicles in the apex. Many Golgi apparatus-derived secreted vesicles start to associate with LlLIM1-stabilized actin filaments and accumulate in the subapical zone, waiting for immediate export to the apical plasma membrane prior to the fast growth phase. LlLIM1 probably functions as an F-actin-bundling protein and coordinates with other oscillators (such as pH and Ca^{2+}) in regulating F-actin remodeling and endomembrane trafficking in periods of slow growth, which is essential for the normal oscillatory growth of pollen tubes. Further studies focusing on the molecular mechanism of actin dynamics in tip-growing cells, and the dynamic distribution and interaction of LlLIM1 with other ABP partners (such as ADF) during oscillatory growth, will be essential and are currently under way in our laboratory.

MATERIALS AND METHODS

Plant Material, Pollen Germination, and Chemicals

Easter lily (*Lilium longiflorum* 'Snow Queen') flower bulbs obtained from a local farm (Foreport Enterprises) were planted in the greenhouse under standard conditions. Mature pollen grains were collected from anthers and dried on a bench for 2 d for further use. Different tissues of mature lily were dissected and collected, and series of developmental stages of anther/pollen were isolated from dissected flower buds ranging from 10 to 150 mm, as described by Gould et al. (1988). To collect in vitro-germinated pollen tubes, pollen grains were placed in germination medium (1.27 mM $CaCl_2$, 0.162 mM H_3BO_3, 0.99 mM KNO_3, and 290 mM Suc, pH 5.2) and collected after different time intervals. Stock solutions of LatB (1 M in DMSO; Sigma-Aldrich) and FM4-64 (1 mM in water; Invitrogen) were divided into aliquots and stored at −20°C. LatB was further diluted to 1 mM and 1 μM with water for the cosedimentation assay and pollen germination assay, respectively. Chemicals without specific notification were purchased from Sigma-Aldrich.

Full-Length cDNA Cloning and Expression Profile Analysis of LlLIM1

The partial sequence of cDNA of *LlLIM1* obtained from clones used for the homemade lily pollen cDNA microarray was used as the template for full-length cDNA cloning. A full-length sequence of cDNA of LlLIM1 was obtained from first-strand cDNA synthesized from lily pollen total RNA (see below) and 5′ and 3′ RACE according to the manufacturer's protocol (SMART RACE cDNA Amplification Kit; Clontech). First-strand cDNA was synthesized from 3 μg of total RNA isolated from different lily tissues, developing and mature anthers, with the Absolutely RNA RT-PCR Miniprep Kit (Stratagene) with oligo(dT) primer, random primers, and Moloney murine leukemia virus reverse transcriptase (Invitrogen). Semiquantitative PCR analyses were performed using the Taq DNA Polymerase RED 2.0 Master Mix kit (1.5 mM $MgCl_2$; Amplicon Transformervej) with lily pollen first-strand cDNA and a gene-specific primer set (5′-CCCCATGGCATTTCAAGGGACAACC-CAG-3′ and 5′-CCCCATGGCAGATCTGGCTGTCTCAGCCACT-3′; Supplemental Table S1) corresponding to the coding sequence of LlLIM1 (nucleotides 205–751). The thermo reaction was conducted with a BiometraR T3 Thermocycler (Whatman Biometra) with the following conditions: 94°C for 5 min; 25 to 35 cycles at 94°C for 1 min, annealing at 55°C to 58°C for 1 min, and 72°C for 1 min; and final elongation at 72°C for 10 min. The resulting PCR products

were separated with a 1% agarose gel containing 0.01% ethidium bromide. To monitor the efficiency of cDNA synthesis by PCR amplification, the housekeeping gene rRNA was used as an internal control for PCR amplification, and a 443-bp fragment was obtained using a specific primer set (5′-GGACAGTCGGGGGCATTCGTAT-3′ and 5′-CCAGACAAATCGCTCCACCAAC-3′).

Recombinant DNA Vector Construction

The plasmids used to transiently express genes in pollen and pollen tubes were derived from a plasmid (*pZM13::GFP*) containing a *GFP* (a gift from Dr. Co-Shine Wang) derived by a maize (*Zea mays*) pollen/pollen tube-specific promoter, *ZM13* (Hamilton et al., 1992), and terminated by the *NOS* terminator. The *LlLIM1* was amplified by PCR using Phusion DNA polymerase (Finnzymes) and was subcloned in the *Nco*I and *Bgl*II sites of *pZM13::GFP* to generate LlLIM1:GFP and GFP:LlLIM1 expression plasmids, respectively. Coding sequences of serial deletions of *LlLIM1* were amplified by PCR with specific primer sets and were subcloned into the *Nco*I site of *pZM13::GFP* to generate series deletions fused to GFP expression plasmids. Full-length and serial deletions of LlLIM1 expression plasmids without GFP were generated by removing *GFP* from gene expression plasmids digested with *Bgl*II and self-ligated. The plasmids used to overexpress 6×His-tagged recombinant protein in *Escherichia coli* were derived from pET30a vector (Novagen). PCR-amplified individual *LlLIM1*, *LlLIM1N*, and *LlLIM1C* were subcloned into the *Nco*I site of pET30a to yield individual expression vectors. Several vectors that express fluorescent marker protein were also generated in this study. To generate an RFP-fused actin marker protein expression vector, *RFP* was amplified from pHD307 (Helling et al., 2006) by PCR and subcloned into the *Xba*I-*Bgl*II sites of *pZM13::GFP* to replace *GFP* and yielded the expression vector pZM1::RFP; the coding sequence of *mTalin* was then amplified from *pLat52::GFP:mTalin* (Dowd et al., 2006) by PCR and subcloned into the *Bgl*II site of *pZM1::RFP*. The coding sequence of the PH domain was amplified from pWEN106 (Helling et al., 2006) by PCR and subcloned into the *Bgl*II site of pZM13::YFP to generate *pZM13::YFP:PH* for tracing PIP2 in living lily pollen tubes. *CYS1:GFP* was amplified from pWEN282 (Helling et al., 2006) by PCR and subcloned into *Xba*I-*Bgl*II sites in pZM13::GFP to replace *GFP* and generate *pZM13::CYS1:GFP* used to localize DAG in living lily pollen tubes. *NAG:CFP* encoding a CFP-fused Golgi network protein was amplified from *pLat52::NAG:CFP* (Dowd et al., 2006) by PCR and subcloned in *Nco*I-*Bgl*II sites in *pZM13::GFP* to replace *GFP* and generate *pZM13::NAG:CFP*. All clones obtained and generated were verified by sequence analysis before use in this study.

High- and Low-Speed Cosedimentation Assays

The 6×His-tagged LlLIM1, LlLIM1N, and LlLIM1C expressed in BL21 were purified with a His-Select Nickel Affinity Gel (Sigma-Aldrich) following procedures described by the manufacturer. The methods of F-actin cosedimentation were modified from Thomas et al. (2006). The purified proteins were buffer exchanged (100 mM NaH_2PO_4 and 10 mM Tris-HCl, pH 7.4) with the use of a 10-K molecular weight cutoff dialysis cassette (Pierce). LlLIM1, LlLIM1N, LlLIM1C, and commercial rabbit skeletal muscle actin filaments (1 mg mL^{-1}; Cytoskeleton) were pelleted at 100,000*g* for 45 min with the Optima TLX ultracentrifuge (Beckman Coulter) at 4°C and dissolved in the same volume of dialysis buffer. Equal amounts of pellet and supernatant samples adding protein sample buffer were analyzed by 12% SDS-PAGE, then stained with Coomassie Brilliant Blue R (Sigma-Aldrich) and used for the following experiments. To determine the F-actin affinity of LlLIM1, LlLIM1N, and LlLIM1C, various amounts of individual proteins (0.5, 1, 2, 4, 8, 12, 24, and 48 μM) were incubated with 4 μM commercially preformed rabbit skeletal muscle actin filaments for 1 h, at 25°C, followed by centrifugation at 100,000*g* for 45 min at 4°C, and were analyzed by SDS-PAGE as described above. High-speed cosedimentation assays were also used to determine the effects of LatB on the F-actin-stabilizing activity of LlLIM1, LlLIM1N, and LlLIM1C. In these experiments, 4 μM commercial rabbit skeletal muscle actin filaments were incubated with various amounts of individual proteins (0, 0.5, 2, 4, 8, 16, and 32 μM) for 1 h at 25°C before the addition of 192 μM LatB or an equal volume of DMSO. After 20 h of treatment with LatB at 25°C, samples were centrifuged at 100,000*g* for 45 min at 4°C and analyzed by SDS-PAGE as described above. In low-speed cosedimentation assays, 0, 0.5, 2, 4, 8, 16, 32, and 64 μM individual LlLIM1, LlLIM1N, or LlLIM1C was incubated with 4 μM commercial rabbit skeletal muscle actin filaments for 1 h, at 25°C, followed by centrifugation at 12,500*g* for 30 min in a microcentrifuge at 4°C, and analyzed by SDS-PAGE as described above. The F-actin sedimentation assay in different pH and [Ca^{2+}] conditions of LlLIM1 was performed as follows: 2 μM LlLIM1 and 2 μM F-actin in nine binding conditions of different pH were buffered by MES and Tris base (pH 6.25, 6.5, 6.75, and 7 in MES buffer; pH 7, 7.25, 7.5, 7.75, and 8 in Tris buffer) for 1 h, these binding mixtures were centrifuged at 100,000*g* to separate pellet and supernatant fractions, and they were analyzed by SDS-PAGE as described above. Commercial EqCal software (Biosoft; www.biosoft.com) was used to calculate the concentration of free Ca^{2+} in different binding solutions containing different amounts of EGTA. Coomassie Brilliant Blue R-stained images from the above experiments were cropped to proper size and contrast enhanced by adjusting brightness and γ setting using image-processing software (Adobe Photoshop).

Transient Gene Expression and Application of LatB and FM4-64 into Cultured Pollen Tubes

Particle bombardment-mediated transient gene expression in lily pollen was modified from Chen et al. (2002). Briefly, 5 mg of pollen grains was rehydrated in germination medium for 30 min and spread evenly onto germination medium-immersed filter paper in a 90-mm petri dish. For the maximal coating capacity, a total amount of 7.5 μg of plasmids was incubated with 1.875-mg gold particles. For each transient expression experiment, 1.875-mg gold particles (1.0 μm) thoroughly coated with plasmids purified using the Geneaid Plasmid Midi Kit (Geneaid) were divided into three parts for consecutive bombardment into pollen grains with the PDS-1000/He Biolistic Particle Delivery System (Bio-Rad) under the following settings: 1,100 p.s.i., 29-mm Hg vacuum, 1-cm gap distance, and 9-cm particle flight distance. Bombarded pollen was immediately washed from filter paper with germination medium, germinated in 2 mL of germination medium in a 3-cm-diameter petri dish with constant shaking at 60 rpm at 30°C for 6 h of incubation to evaluate the localization of selected molecules or for 12 h of incubation to examine in vitro pollen tube growth assay by fluorescent laser confocal microscopy. To analyze whether LlLIM1-, LlLIM1N-, and LlLIM1C-overexpressing pollen can be resistant to a LatB-induced germination defect, different amounts of LatB (10, 20, and 30 nM) and a 3×10^{-5} dilution of DMSO in water (the final DMSO concentration in 30 nM LatB [v/v]) were added to the germination medium containing bombarded pollen. After 12 h of culture, images of pollen/pollen tubes in a 30-mm-diameter petri dish with GFP signal were recorded by fluorescence microscopy (see below). To visualize internal membranes, FM4-64 was added to a final concentration of 10 μM in 500 μL of cultured medium containing bombarded pollen/pollen tubes after 6 h of incubation prior to fluorescence microscopy observation; image recording involved the use of confocal microscopy (see below) followed by 30 min of incubation in the dark at room temperature.

Microscopy and Image Analysis

For in vitro pollen tube growth assay, germinating 12-h pollen tubes showing GFP signal were observed directly with an epifluorescence microscope (BX51; Olympus) to record images by cooling CCD (DP70; Olympus) through 4× and 10× lenses (UPlanFI; Olympus) and GFP filter. The lengths of pollen tubes with GFP signal on the digital low-magnification images (5× lens) were measured with ImageJ software (http://rsb.info.nih.gov/ij/) and were analyzed by SPSS (SPSS) and Excel (Microsoft).

For confocal laser scanning fluorescence microscopy, 140 μL of bombarded pollen tubes cultured for 6 h was allowed to settle onto the cover slide before mounting with a coverslip and sealing. An LSM510 META confocal microscope (Carl Zeiss) was used to record high-resolution confocal sections through a 63× lens (C-Apochroat 63×/1.2 water immersion; Carl Zeiss). A 488-nm laser line and a 500- to 530-nm band-pass emission filter, or a 543-nm laser line and a 560-nm long-pass emission filter, were used for GFP or RFP imaging, respectively. Projected images was obtained by recoding series of confocal images from the top to the bottom section of individual pollen tubes lying flat on the coverslip surface at less Z-scaling estimated with an optima pinhole diameter 63× lens (Fig. 3C; Supplemental Fig. S4). GFP and RFP coimaging was performed in the multitracking mode (Fig. 2). A 488-nm laser line and a 650- to 710-nm band-pass emission filter were used for FM4-64 imaging. Time-lapse images of GFP and FM4-64 were recorded with 9-s intervals in single-tracking mode (Figs. 5 and 7). To measure growth rates, the distance traveled by the apex of individual pollen tubes during 9 s was determined using ImageJ software, and growth rate was calculated through

growth distance data using Excel (Figs. 5 and 7). A 488-nm laser line and a 500- to 550-nm band-pass emission filter were used for YFP imaging (Supplemental Fig. S5). CFP images were recorded with a 458-nm laser line and a 480- to 520-nm band-pass emission filter. For GFP and CFP coimaging, multitracking mode was used by recording GFP and CFP images, respectively (Fig. 7). All images were recorded at 1,024 × 1,024 pixels using line 2 averaged scanning. Confocal images were cropped to the proper size and were contrast enhanced by adjusting brightness and γ setting using Adobe Photoshop.

Accession Number

The cDNA sequence for LlLIM1 was deposited in GenBank under accession number EU186001.

Supplemental Data

The following materials are available in the online version of this article.

Supplemental Figure S1. The sequence and the estimated length of full-length *LlLIM1* transcript.

Supplemental Figure S2. Expression of serial deletion of LIM counterparts of LlLIM1 in elongating pollen tubes showed various degrees of effects on F-actin decoration and pollen tube growth.

Supplemental Figure S3. Projective images of elongating pollen tubes containing the variants of deleted LIM counterparts of LlLIM1 shown in Supplemental Figure S2B.

Supplemental Figure S4. Cosedimentation assays revealed direct binding to promote F-actin bundling by N-half (LlLIM1N) and C-half (LlLIM1C) recombinant LlLIM1 proteins.

Supplemental Figure S5. Overexpression of LlLIM1 in pollen stabilized and protected F-actin from depolymerization by LatB.

Supplemental Figure S6. LlLIM1 overexpression impaired pollen tube growth by disturbing actin dynamics and accumulating abundant FM4-64-labeled vesicles at the subapex of elongating pollen tubes.

Supplemental Figure S7. LlLIM1 overexpression disturbed the apical membrane localization of signal molecule PIP2 in elongating pollen tubes.

Supplemental Table S1. Nucleotide sequences of primer sets used in this study.

Supplemental Movie S1. Dynamic imaging of GFP and FM4-64 in pollen tubes overexpressing GFP.

Supplemental Movie S2. Dynamic imaging of LlLIM1:GFP and FM4-64 in pollen tubes overexpressing LlLIM1:GFP shows growth.

Supplemental Movie S3. Dynamic imaging of LlLIM1:GFP and FM4-64 in pollen tubes overexpressing LlLIM1:GFP shows greatly reduced growth.

Supplemental Movie S4. Dynamic imaging of LlLIM1:GFP in pollen tubes moderately expressing LlLIM1:GFP.

ACKNOWLEDGMENTS

We thank Mei-Jane Fang for assistance with confocal microscopy. We also express our grateful appreciation to Drs. Alice Y. Cheung, Simon Gilroy, Benedikt Kost, and Co-Shine Wang for sharing their treasured plasmids with us.

Received March 2, 2008; accepted May 8, 2008; published May 14, 2008.

LITERATURE CITED

Allwood EG, Anthony RG, Smertenko AP, Reichelt S, Drobak BK, Doonan JH, Weeds AG, Hussey PJ (2002) Regulation of the pollen-specific actin-depolymerizing factor LlADF1. Plant Cell **14:** 2915–2927

Arber S, Barbayannis FA, Hanser H, Schneider C, Stanyon CA, Bernard O, Caroni P (1998) Regulation of actin dynamics through phosphorylation of cofilin by LIM-kinase. Nature **393:** 805–809

Arber S, Caroni P (1996) Specificity of single LIM motifs in targeting and LIM/LIM interactions in situ. Genes Dev **10:** 289–300

Arnaud D, Déjardin A, Leplé JC, Lesage-Descauses MC, Pilate G (2007) Genome-wide analysis of LIM gene family in *Populus trichocarpa*, Arabidopsis, and *Oryza sativa*. DNA Res **14:** 103–116

Baltz R, Domon C, Pillay DT, Steinmetz A (1992) Characterization of a pollen-specific cDNA from sunflower encoding a zinc finger protein. Plant J **2:** 713–721

Baltz R, Schmit AC, Kohnen M, Hentges F, Steinmetz A (1999) Differential localization of the LIM domain protein PLIM-1 in microspores and mature pollen grains from sunflower. Sex Plant Reprod **12:** 60–65

Cardenas L, Lovy-Wheeler A, Wilsen KL, Hepler PK (2005) Actin polymerization promotes the reversal of streaming in the apex of pollen tubes. Cell Motil Cytoskeleton **61:** 112–127

Chen CY, Wong EI, Vidali L, Estavillo A, Hepler PK, Wu HM, Cheung AY (2002) The regulation of actin organization by actin-depolymerizing factor in elongating pollen tubes. Plant Cell **14:** 2175–2190

Chen T, Teng N, Wu X, Wang Y, Tang W, Samaj J, Baluska F, Lin J (2007) Disruption of actin filaments by latrunculin B affects cell wall construction in *Picea meyeri* pollen tube by disturbing vesicle trafficking. Plant Cell Physiol **48:** 19–30

Cheung AY, Wu HM (2004) Overexpression of an *Arabidopsis* formin stimulates supernumerary actin cable formation from pollen tube cell membrane. Plant Cell **16:** 257–269

Cheung AY, Wu HM (2008) Structural and signaling networks for the polar cell growth machinery in pollen tubes. Annu Rev Plant Physiol Plant Mol Biol **59:** 547–572

Dettmer J, Hong-Hermesdorf A, Stierhof YD, Schumacher K (2006) Vacuolar H^+-ATPase activity is required for endocytic and secretory trafficking in *Arabidopsis*. Plant Cell **18:** 715–730

Dixit R, Cyr R (2002) Golgi secretion is not required for marking the preprophase band site in cultured tobacco cells. Plant J **29:** 99–108

Dowd PE, Coursol S, Skirpan AL, Kao TH, Gilroy S (2006) Petunia phospholipase C1 is involved in pollen tube growth. Plant Cell **18:** 1438–1453

Dutta R, Robinson KR (2004) Identification and characterization of stretch-activated ion channels in pollen protoplasts. Plant Physiol **135:** 1398–1406

Eliasson A, Gass N, Mundel C, Baltz R, Krauter R, Evrard JL, Steinmetz A (2000) Molecular and expression analysis of a LIM protein gene family from flowering plants. Mol Gen Genet **264:** 257–267

Fan X, Hou J, Chen X, Chaudhry F, Staiger CJ, Ren H (2004) Identification and characterization of a Ca^{2+}-dependent actin filament-severing protein from lily pollen. Plant Physiol **136:** 3979–3989

Feijó JA, Sainhas J, Hackett GR, Kunkel JG, Hepler PK (1999) Growing pollen tubes possess a constitutive alkaline band in the clear zone and a growth-dependent acidic tip. J Cell Biol **144:** 483–496

Gibbon BC, Kovar DR, Staiger CJ (1999) Latrunculin B has different effects on pollen germination and tube growth. Plant Cell **11:** 2349–2363

Gould IM, Reeves I, Chauhan N (1988) Novel plate culture method to improve the microbiological diagnosis of peritonitis in patients on continuous ambulatory peritoneal dialysis. J Clin Microbiol **26:** 1687–1690

Grubinger M, Gimona M (2004) CRP2 is an autonomous actin-binding protein. FEBS Lett **557:** 88–92

Gungabissoon RA, Khan S, Hussey PJ, Maciver SK (2001) Interaction of elongation factor 1a from *Zea mays* (ZmEF-1a) with F-actin and interplay with the maize actin severing protein, ZmADF3. Cell Motil Cytoskeleton **49:** 104–111

Hamilton DA, Roy M, Rueda J, Sindhu RK, Sanford J, Mascarenhas JP (1992) Dissection of a pollen-specific promoter from maize by transient transformation assays. Plant Mol Biol **18:** 211–218

Helling D, Possart A, Cottier S, Klahre U, Kost B (2006) Pollen tube tip growth depends on plasma membrane polarization mediated by tobacco PLC3 activity and endocytic membrane recycling. Plant Cell **18:** 3519–3534

Hepler PK, Vidali L, Cheung AY (2001) Polarized cell growth in higher plants. Annu Rev Cell Dev Biol **17:** 159–187

Holdaway-Clarke TL, Feijo JA, Hackett GR, Kunkel JG, Hepler PK (1997) Pollen tube growth and the intracellular cytosolic calcium gradient oscillate in phase while extracellular calcium influx is delayed. Plant Cell **9:** 1999–2010

Holdaway-Clarke TL, Weddle NM, Kim S, Robi A, Parris C, Kunkel JG, Hepler PK (2003) Effect of extracellular calcium, pH and borate on

growth oscillations in *Lilium formosanum* pollen tubes. J Exp Bot **54:** 65–72

Hörmanseder K, Obermeyer G, Foissner I (2005) Disturbance of endomembrane trafficking by brefeldin A and calyculin A reorganizes the actin cytoskeleton of *Lilium longiflorum* pollen tubes. Protoplasma **227:** 25–36

Huang S, Blanchoin L, Chaudhry F, Franklin-Tong VE, Staiger CJ (2004) A gelsolin-like protein from *Papaver rhoeas* pollen (PrABP80) stimulates calcium-regulated severing and depolymerization of actin filaments. J Biol Chem **279:** 23364–23375

Huang S, Robinson RC, Gao LY, Matsumoto T, Brunet A, Blanchoin L, Staiger CJ (2005) *Arabidopsis* VILLIN1 generates actin filament cables that are resistant to depolymerization. Plant Cell **17:** 486–501

Hussey PJ, Ketelaar T, Deeks MJ (2006) Control of the actin cytoskeleton in plant cell growth. Annu Rev Plant Biol **57:** 109–125

Ketelaar T, Anthony RG, Hussey PJ (2004) Green fluorescent protein-mTalin causes defects in actin organization and cell expansion in Arabidopsis and inhibits actin depolymerizing factor's actin depolymerizing activity in vitro. Plant Physiol **136:** 3990–3998

Khurana T, Khurana B, Noegel AA (2002) LIM proteins: association with the actin cytoskeleton. Protoplasma **219:** 1–12

Kost B, Spielhofer P, Chua NH (1998) A GFP-mouse talin fusion protein labels plant actin filaments in vivo and visualizes the actin cytoskeleton in growing pollen tubes. Plant J **16:** 393–401

Kovar DR, Drobak BK, Staiger CJ (2000) Maize profilin isoforms are functionally distinct. Plant Cell **12:** 583–598

Lovy-Wheeler A, Cardenas L, Kunkel JG, Hepler PK (2007) Differential organelle movement on the actin cytoskeleton in lily pollen tubes. Cell Motil Cytoskeleton **64:** 217–232

Lovy-Wheeler A, Kunkel JG, Allwood EG, Hussey PJ, Hepler PK (2006) Oscillatory increases in alkalinity anticipate growth and may regulate actin dynamics in pollen tubes of lily. Plant Cell **18:** 2182–2193

Lovy-Wheeler A, Wilsen KL, Baskin TI, Hepler PK (2005) Enhanced fixation reveals the apical cortical fringe of actin filaments as a consistent feature of the pollen tube. Planta **221:** 95–104

Malhó R (2006) The pollen tube. *In* R Malhó, ed, Plant Cell Monographs, Vol 3. Springer, Berlin/Heidelberg, pp 1–13

Maul RS, Song Y, Amann KJ, Gerbin SC, Pollard TD, Chang DD (2003) EPLIN regulates actin dynamics by cross-linking and stabilizing filaments. J Cell Biol **160:** 399–407

Mundel C, Baltz R, Eliasson A, Bronner R, Grass N, Krauter R, Evrard JL, Steinmetz A (2000) A LIM-domain protein from sunflower is localized to the cytoplasm and/or nucleus in a wide variety of tissues and is associated with the phragmoplast in dividing cells. Plant Mol Biol **42:** 291–302

Nakayasu T, Yokota E, Shimmen T (1998) Purification of an actin-binding protein composed of 115-kDa polypeptide from pollen tubes of lily. Biochem Biophys Res Commun **249:** 61–65

Oancea E, Teruel MN, Quest AF, Meyer T (1998) Green fluorescent protein (GFP)-tagged cysteine-rich domains from protein kinase C as fluorescent indicators for diacylglycerol signaling in living cells. J Cell Biol **140:** 485–498

Parton RM, Fischer-Parton S, Watahiki MK, Trewavas AJ (2001) Dynamics of the apical vesicle accumulation and the rate of growth are related in individual pollen tubes. J Cell Sci **114:** 2685–2695

Picton JM, Steer MW (1983) Membrane recycling and the control of secretory activity in pollen tubes. J Cell Sci **63:** 303–310

Pierson ES, Miller DD, Callaham DA, van Aken J, Hackett G, Hepler PK (1996) Tip-localized calcium entry fluctuates during pollen tube growth. Dev Biol **174:** 160–173

Šamaj J, Baluška F, Voigt B, Schlicht M, Volkmann D, Menzel D (2004) Endocytosis, actin cytoskeleton, and signaling. Plant Physiol **135:** 1150–1161

Šamaj J, Müller J, Beck M, Böhm N, Menzel D (2006) Vesicular trafficking, cytoskeleton and signalling in root hairs and pollen tubes. Trends Plant Sci **11:** 594–600

Schmeichel KL, Beckerle MC (1997) Molecular dissection of a LIM domain. Mol Biol Cell **8:** 219–230

Sheahan MB, Staiger CJ, Rose RJ, McCurdy DW (2004) A green fluorescent protein fusion to actin-binding domain 2 of Arabidopsis fimbrin highlights new features of a dynamic actin cytoskeleton in live plant cells. Plant Physiol **136:** 3968–3978

Staiger CJ, Blanchoin L (2006) Actin dynamics: old friends with new stories. Curr Opin Plant Biol **9:** 554–562

Thaler JP, Lee SK, Jurata LW, Gill GN, Pfaff SL (2002) LIM factor Lhx3 contributes to the specification of motor neuron and interneuron identity through cell-type-specific protein-protein interactions. Cell **110:** 237–249

Thomas C, Hoffmann C, Dieterle M, Van Troys M, Ampe C, Steinmetz A (2006) Tobacco WLIM1 is a novel F-actin binding protein involved in actin cytoskeleton remodeling. Plant Cell **18:** 2194–2206

Thomas C, Moreau F, Dieterle M, Hoffmann C, Gatti S, Hofmann C, Van Troys M, Ampe C, Steinmetz A (2007) The LIM domains of WLIM1 define a new class of actin bundling modules. J Biol Chem **282:** 33599–33608

Tominaga M, Yokota E, Vidali L, Sonobe S, Hepler PK, Shimmen T (2000) The role of plant villin in the organization of the actin cytoskeleton, cytoplasmic streaming and the architecture of the transvacuolar strand in root hair cells of Hydrocharis. Planta **210:** 836–843

Tran TC, Singleton C, Fraley TS, Greenwood JA (2005) Cysteine-rich protein 1 (CRP1) regulates actin filament bundling. BMC Cell Biol **6:** 45

Vidali L, Hepler PK (2001) Actin and pollen tube growth. Protoplasma **215:** 64–76

Voigt B, Timmers AC, Samaj J, Muller J, Baluska F, Menzel D (2005) GFP-FABD2 fusion construct allows in vivo visualization of the dynamic actin cytoskeleton in all cells of Arabidopsis seedlings. Eur J Cell Biol **84:** 595–608

Wadman IA, Osada H, Grutz GG, Agulnick AD, Westphal H, Forster A, Rabbitts TH (1997) The LIM-only protein Lmo2 is a bridging molecule assembling an erythroid, DNA-binding complex which includes the TAL1, E47, GATA-1 and Ldb1/NLI proteins. EMBO J **16:** 3145–3157

Wang YS, Motes CM, Mohamalawari DR, Blancaflor EB (2004) Green fluorescent protein fusions to Arabidopsis fimbrin 1 for spatio-temporal imaging of F-actin dynamics in roots. Cell Motil Cytoskeleton **59:** 79–93

Weiskirchen R, Gunther K (2003) The CRP/MLP/TLP family of LIM domain proteins: acting by connecting. Bioessays **25:** 152–162

Wilsen KL, Lovy-Wheeler A, Voigt B, Menzel D, Kunkel JG, Hepler PK (2006) Imaging the actin cytoskeleton in growing pollen tubes. Sex Plant Reprod **19:** 51–62

Yokota E, Muto S, Shimmen T (2000) Calcium-calmodulin suppresses the filamentous actin-binding activity of a 135-kilodalton actin-bundling protein isolated from lily pollen tubes. Plant Physiol **123:** 645–654

Yokota E, Takahara K, Shimmen T (1998) Actin-bundling protein isolated from pollen tubes of lily: biochemical and immunocytochemical characterization. Plant Physiol **116:** 1421–1429

Yokota E, Tominaga M, Mabuchi I, Tsuji Y, Staiger CJ, Oiwa K, Shimmen T (2005) Plant villin, lily P-135-ABP, possesses G-actin binding activity and accelerates the polymerization and depolymerization of actin in a Ca^{2+}-sensitive manner. Plant Cell Physiol **46:** 1690–1703

Yokota E, Vidali L, Tominaga M, Tahara H, Orii H, Morizane Y, Hepler PK, Shimmen T (2003) Plant 115-kDa actin-filament bundling protein, P-115-ABP, is a homologue of plant villin and is widely distributed in cells. Plant Cell Physiol **44:** 1088–1099